Hindawi
Geofluids
Volume 2024, Article ID 1235792, 22 pages
https://doi.org/10.1155/2024/1235792

Research Article

Reservoir Quality, Lithotype Assessment, and Geochemical Source Rock Analysis: Insights from Well Logs and Pyrolysis Data, Karama Field, North-Western Desert, Egypt

Mahmoud Mamdouh,[1] **Mohamed Reda**,[1] **Abdelmoneam Raef**,[2] **M. Y. Zein El Din**,[1] **Tharwat H. Abdelhafeez**,[1] **and Mansour H. Al-Hashim**[3]

[1]*Al-Azhar University, Faculty of Science, Geology Department, Cairo, Egypt*
[2]*Department of Geology, Kansas State University, Manhattan, Kansas, USA*
[3]*Department of Geology and Geophysics, College of Science, King Saud University, Riyadh 11451, Saudi Arabia*

Correspondence should be addressed to Abdelmoneam Raef; abraef@ksu.edu

Received 3 January 2024; Revised 29 January 2024; Accepted 10 February 2024; Published 6 March 2024

Academic Editor: Muhammad Tayyab Naseer

Reservoir characteristics and source rock geochemistry are essential for petroleum system investigation as they reveal reservoir quality and hydrocarbon generation capability, respectively. The primary Karama oil field reservoir of Abu El Gharadig Basin is the limestone-sand-shale Abu Roash G (AR/G) Member. This study examines AR/G, analyzes source rocks for maturity and organic elements, and defines the main reservoir lithotypes and evaluates reservoir properties. Five well log datasets and an AR/F pyrolysis analysis on another well were used in this study to characterize the AR/G's 168-foot effective thickness and assess the AR/F source-rock maturation. The effective porosity is up to 30%. The highest shale concentration was 24% in central and western parts of the field. Therefore, drilling development wells in this area, especially east and north, demands caution. The composition and vertical and lateral lithofacies variations of the defined reservoir in the Karama field region are a significant control of its petrophysical properties. The pyrolysis of AR/F revealed 1.32–5.84% content of organic matter. That content qualifies AR/F as a hydrocarbon source if thermal maturity is reached. Type I and type II kerogen in the Abu Roash F Member suggests oil production. The Abu Roash G Member and Upper Bahariya (UB) formation produce oil and gas due to their own type II and III kerogen. GC biomarker data suggests that the research area is predominantly maritime, with most samples showing environmental degradation. The area under consideration has one reservoir, AR/G, and three members of source rocks in AR/F&G and UB. AR/G electrofacies revealed various lithotypes and flow units.

1. Introduction

The assessment of reservoir quality is of paramount importance in the exploration and extraction of hydrocarbon reserves, as it offers significant insights into the economic feasibility and productivity of oil and gas reservoirs. The assessment of reservoir quality involves many reservoir attributes like porosity, permeability, and fluid saturation, essential to evaluating the potential of hydrocarbon accumulation and assessing the recoverable reserves [1–12].

The utilization of geochemical analysis is of great significance within the domain of hydrocarbon exploration and production, as it offers vital parameters pertaining to the quality of hydrocarbon source rocks and level of organic matter maturation [10, 13–16]. Furthermore, the utilization of geochemical analysis plays a crucial role in comprehending the depositional environment, diagenetic processes, and interactions between fluids and rocks [10, 14, 17]. These aspects are of utmost importance in reservoir modeling, the anticipation of reservoir heterogeneity, and the development of techniques for enhanced oil recovery (EOR).

Well logs provide a comprehensive geophysical account of subsurface formations, supplying essential information regarding lithological attributes, porosity, permeability, and

other significant rock properties [8–10, 18–20]. When combined with Rock-Eval pyrolysis, a method that involves controlled heating of rock samples to measure their organic composition and thermal maturity, researchers can evaluate the potential for hydrocarbon generation in source rocks [8, 10, 21–23]. In addition, the analysis of biomarker data involves the examination of specific chemical compounds found in rock samples and their comparison to those found in generated oils. This analysis aids in the determination of the origins and environmental conditions under which hydrocarbons were formed [8, 17, 24, 25]. The utilization of a diverse range of methods not only facilitates the identification of possible reservoirs but also contributes to the prediction of the characteristics and types of extractable hydrocarbons, thus guiding decision-making processes in the fields of exploration and production.

The Karama oil field is in the eastern portion of the East Bahariya Concession (EBC), in the northern section of Egypt's Western Desert, in the Abu Gharadig Basin. The Karama oil field is a component of the basin's southeast side. Since several oil and gas discoveries have been reported within its thick marine Cretaceous sequence, this basin is currently thought to be the most promising basin [4, 7, 9, 15, 26–28]. About 185 kilometers from 6th of October city, the area under investigation is situated between latitudes 29°32′25.45″N and 29°34′36.98″N and longitudes 29°29′37.78″E and 29°32′04.42″E (Figure 1(a)). Hydrocarbon production is almost entirely concentrated in Cretaceous carbonate and clastic reservoirs [26]. The southeast Karama oil field was discovered by the Qarun Petroleum Company in 2002 after going through several stages of exploration and abandonment.

The primary objective of the present study is to conduct a thorough evaluation of the reservoir strata of the Upper Cretaceous epoch, as it represents a significant reservoir formation within the study region. The examination of the petrophysical characteristics of the reservoir is widely recognized as a fundamental component within the oil and gas sector. This analysis offers crucial insights on the reservoir's quality, heterogeneities, and productivity, hence playing a pivotal role in hydrocarbon field development decisions. The assessment of reservoir quality can be conducted, utilizing various geophysical datasets that are readily accessible. This evaluation encompasses various reservoir attributes, with particular emphasis on the effective thickness ratio, effective porosity, and water saturation.

The subsequent section of the project is aimed at conducting a comprehensive geochemical evaluation of the Upper Cretaceous source rocks (AR/F, AR/G, and U. Bahariya), examining their potential as a source rock within the Karam oil field located in the northern Western Desert of Egypt. This phase of the study will rely on a geochemical dataset to assess the hydrocarbon sourcing potential of the Abu Roash and Bahariya formations. This evaluation will enable us to determine the suitability of these rock formations for oil or gas extraction. Consequently, we will be able to identify the specific source rocks that contribute significantly to the Abu Roash G Member, which serves as the primary reservoir within the specified geographic area.

In this case study, the integration of the evaluated petrophysical properties of the Upper Cretaceous reservoir rock, specifically the Abu Roash G Member, along with the findings from the geochemical evaluation of the potential source rocks (Abu Roash and Bahariya formations), is of strong relevance not only for Karama field but also to the exploration and development in other concessions of the northern Western Desert of Egypt, where the Upper Cretaceous formations are of interest. This study provides evaluation of the quality and prospectivity of the petroleum system in the region. Consequently, it greatly facilitates decision-making processes concerning development strategies and future drilling initiatives for enhanced exploration endeavors.

2. Regional Geology

2.1. Lithostratigraphic Setting and Tectonic History. The stratigraphic column (Figure 2) represents the geological sequence of the Western Desert in Egypt. This sequence comprises a considerable span of time, ranging from the Precambrian era to Recent, according to Abu El-Naga [29], Reda et al. [10], Bakr et al. [4], and El-Qalamoshy et al. [7].

Four major sedimentary cycles with strong southerly transgressions occurred throughout the Carboniferous, Late Jurassic, Middle and Late Cretaceous, Middle Miocene, and Pliocene. Permo-Triassic and Early Jurassic geological periods had maximal northward regressive phases. These stages lasted throughout the Early Cretaceous and Late Eocene through Oligocene. The late Miocene saw a last phase [6]. This study analyzes the Upper Cretaceous stratigraphy, focusing on the AR\G Member as the principal reservoir in the Karama oil field.

The Alam El Bueib Formation, with its sandstone facies and shales, is one of the Early Cretaceous formations. Over the Jurassic Masajid Formation, the Alamein Dolomite, Dahab Shale, and Kharita Sandstone are in conformable sequence. Unconformably overlaying the Kharita Sandstone, the Bahariya Formation is predominantly argillaceous. However, the Late Cretaceous Abu Roash Formation of sandstone, limestone, and shale overlies the Bahariya Formation. The Late Cretaceous Khoman Chalk Formation unconformably overlies the Abu Roash Formation and underlies the Paleocene/Eocene Appollonia Limestone Formation [4, 7, 9, 10, 27].

The Middle Jurassic Khatatba Formation (consisting of a fluvio-deltaic sequence of the fossilliferous clastics) and Masajid Formation (composed of massive carbonate sediments) unconformably overlie the Paleozoic formations, which are primarily characterized by argillaceous sandstone. The Early Cretaceous Alam El Bueib Formation, which includes sandstone facies interbedded with shales, Alamein Dolomite, Dahab Shale, and Kharita Sandstone, conformably overlies the Jurassic Masajid Formation. Kharita Sandstone is unconformably overlain by the Bahariya Formation, which is primarily argillaceous sandstone, while the Late Cretaceous Abu-Roash Formation, which is limestone, shale, and sandstone, conformably overlies it. The Late Cretaceous Khoman Chalk Formation unconformably overlies the Paleocene–Eocene Abu-Roash and Appolonia

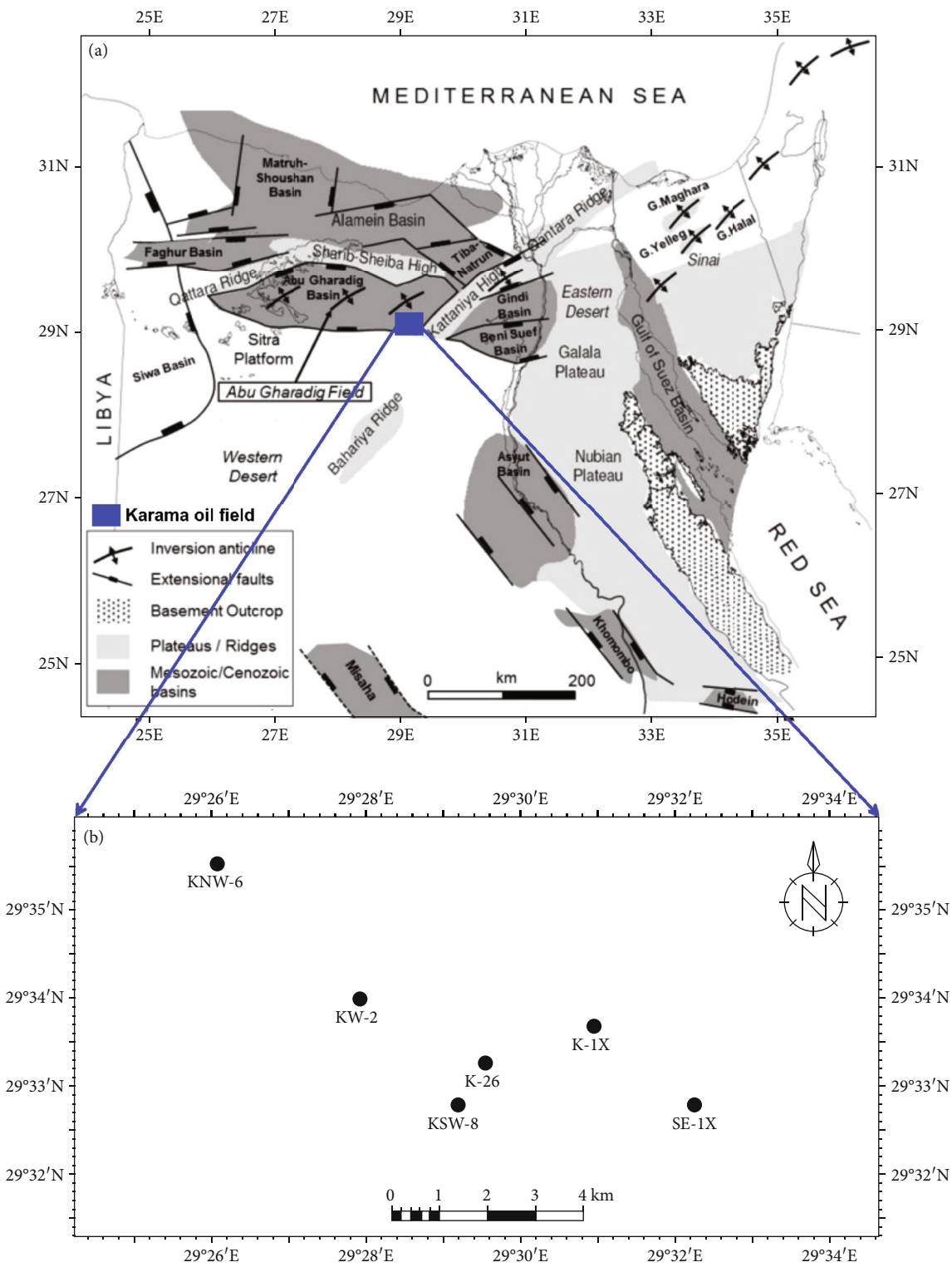

Figure 1: (a) Mesozoic and Cenozoic basins in Egypt (modified after [57–59]; Upper Egypt basins added after [60]); the blue cube shape represents the area of study. (b) The distribution of the available wells in the Karama oil field.

Limestone Formations. The Oligocene-aged Dabaa Shale, Miocene Moghra and Marmarica layers, and Pliocene-Recent sandstone layers (Kurkar and El Hammam) consistently overlie the Appolonia Formation [9].

2.2. Structure Setting. In-depth understanding of the structural context of the Abu Gharadig Basin holds paramount importance in facilitating hydrocarbon exploration and production endeavors. This understanding focuses on the

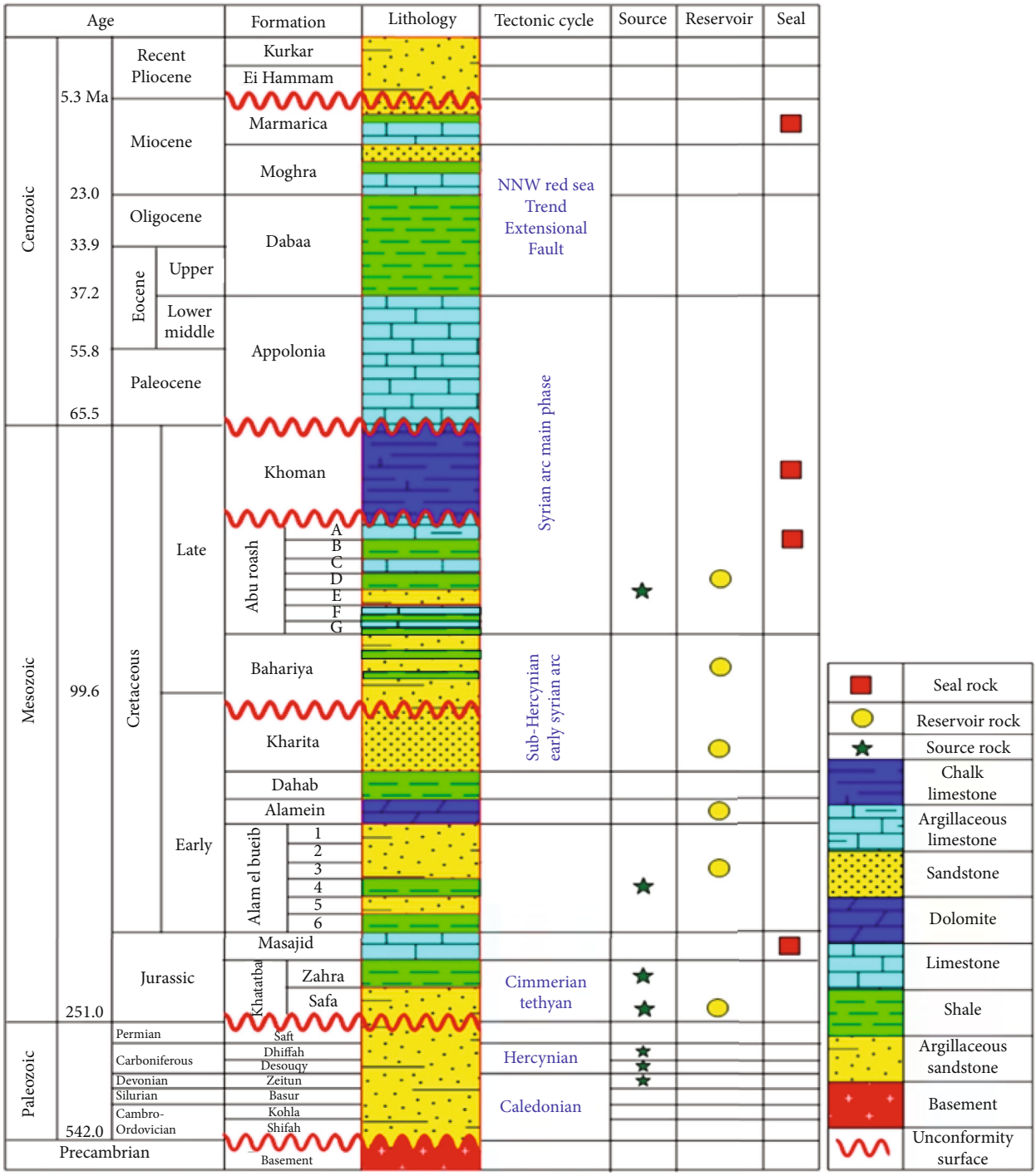

Figure 2: Geologic stratigraphic column of the Abu Gharadig Basin in the North-Western Desert, Egypt, modified after [10, 61].

identification of geographically advantageous regions for the establishment of reservoirs, the identification of prospective hydrocarbon traps, and the optimization of well sitting. Furthermore, the intricate nature of geological structures plays a crucial role in leveraging an informed assessment of the reliability of reservoir seals and forecasting the routes by which fluids may migrate [30, 31].

The Abu Gharadig Basin, situated in the North-Western Desert of Egypt, demonstrates a multifaceted structural configuration that holds noteworthy ramifications for the discovery and production of hydrocarbons in the area. The basin has distinct geological features such as fault networks, folds, and flexures, which have played a significant role in shaping the distribution and containment of hydrocarbons inside the reservoirs.

The predominant elements of the structural framework of the Abu Gharadig Basin are represented by a network of faults that trend in a northwest-southeast direction,

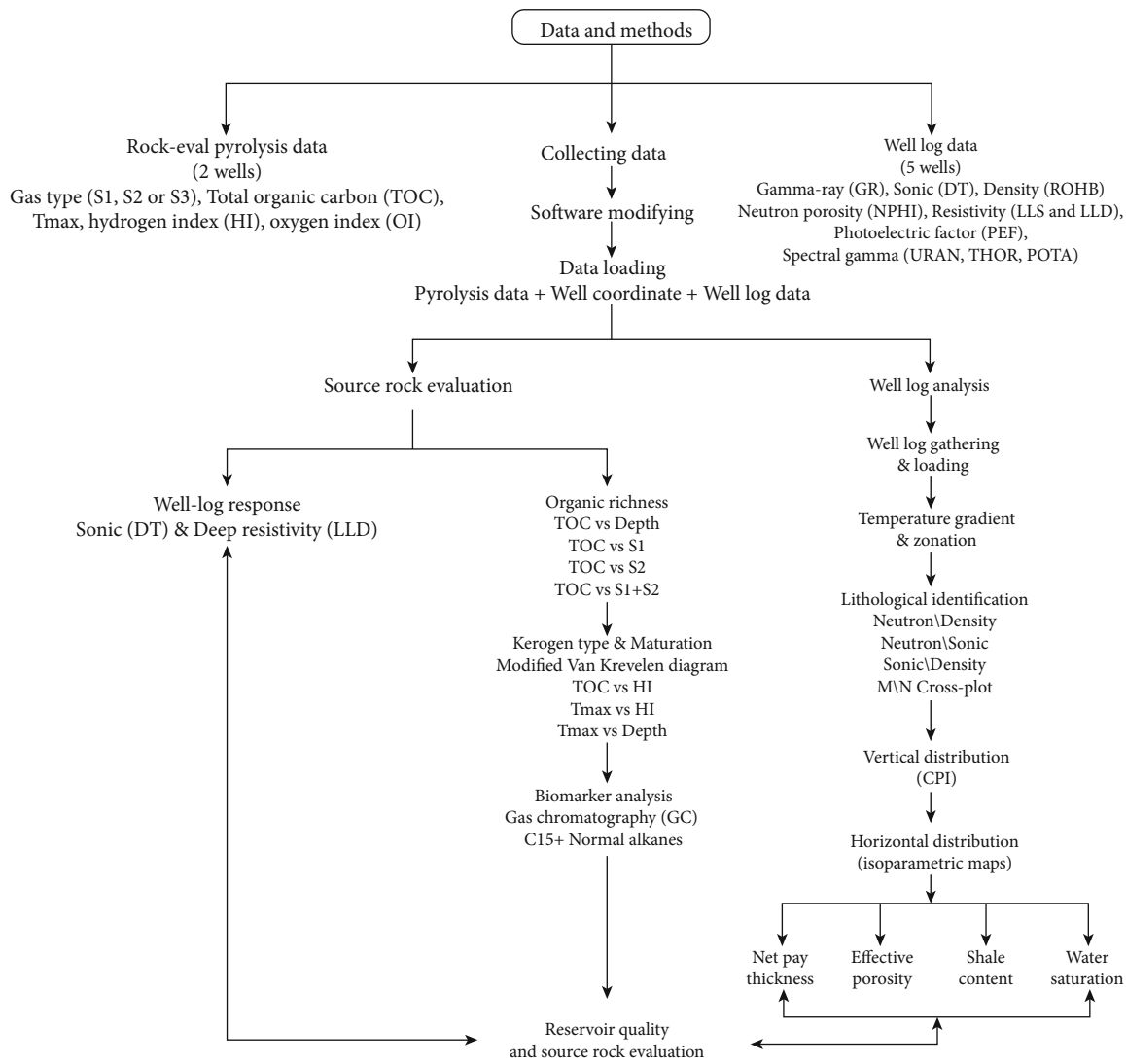

Figure 3: Schematic diagram showing the detailed workflow used in the study area.

complemented by another set of faults that trend in a northeast-southwest direction. The presence of these geological faults has led to the formation of a sequence of horst and graben structures, which in turn have caused the basin to be divided into discrete fault blocks. The fault blocks demonstrate varieties of geometric characteristics, fault activity patterns, and history of subsidence, which therefore result in variations in the quality of reservoirs and their production (e.g., [4, 7, 9, 32]).

Western Desert fault trends and sedimentary basins are shown in Figure 1(a). Three tectonic episodes affected the North-Western Desert, e.g., [33]. The first tectonic event produced NW or WNW structures during the Pre-Cambrian and revived during the Late Tertiary and Early Quaternary, the second episode may have been of Cretaceous age and has an ENE trend, and the third tectonic episode produced NW-SE (Suez) and NNE (Aqaba) structures. The Northern-Western Desert, where multiple hydrocarbon source formations have been found, appears to have undergone various phases of deformation in the Late Cretaceous, post-Middle Eocene, and Middle Miocene due to its tectonic development, according to Moustafa et al. [32]; subsurface data showed Early Mesozoic normal faulting.

3. Data and Methods

The objective of this study is to analyze the reservoir quality and productivity of the Abu Roash G Member reservoir, as well as conduct a thorough evaluation of the source rocks in the Karama oil field, specifically the Abu Roash F and G Members and the Upper Bahariya Formation. To accomplish this objective, the study was bifurcated into two primary components: the geophysical assessment of the reservoir and subsequently the geochemical assessment of the source rocks. Figure 3 provides the workflow of this study.

To identify the main producing zones in the research region using petrophysical techniques, it is important to identify the reservoir characteristics for the chosen reservoirs. The geophysical assessment of the reservoir layer

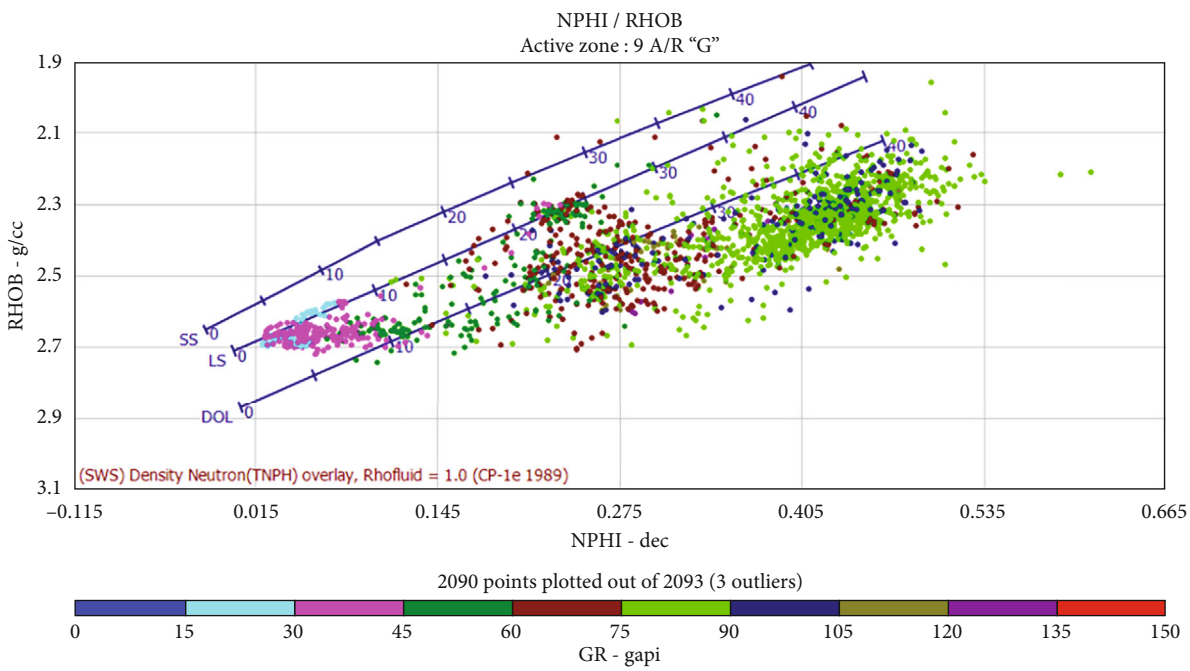

(a)

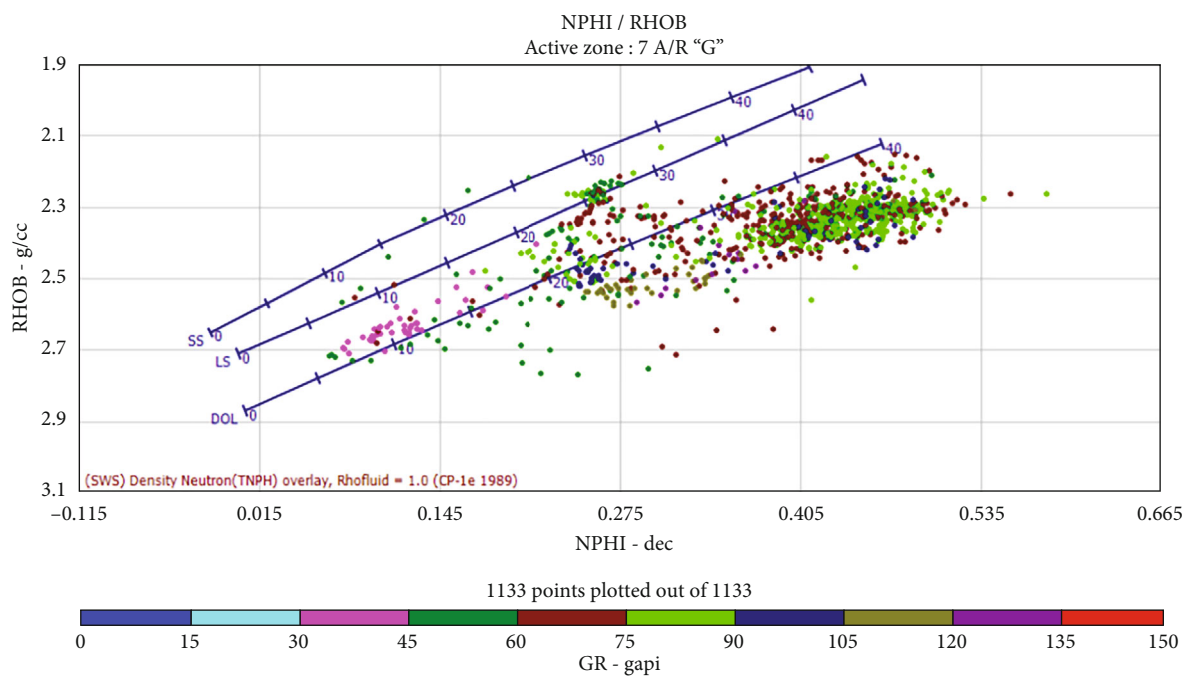

(b)

Figure 4: Continued.

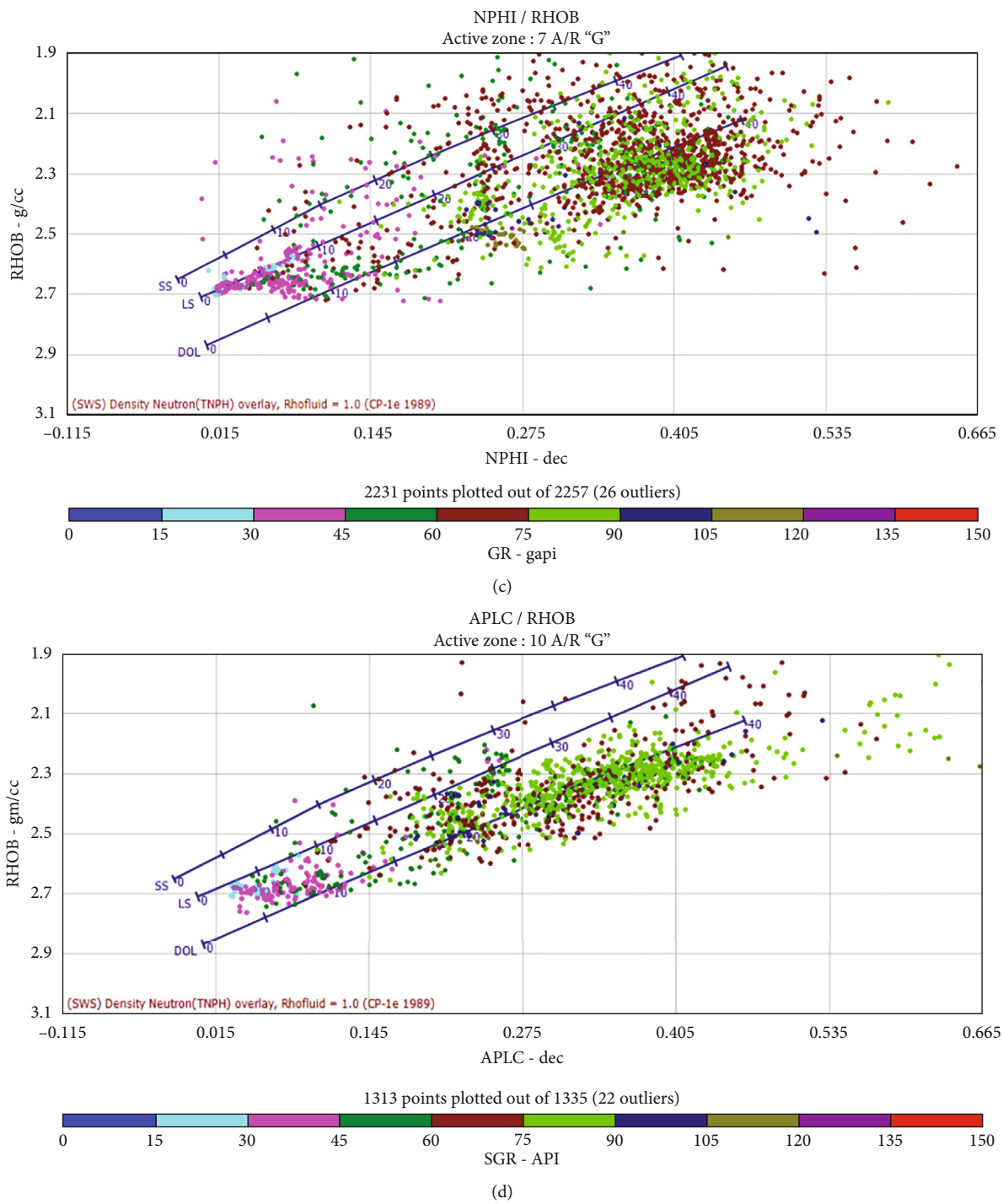

Figure 4: Lithological identification neutron-density cross-plots for the Abu Roash (G) Member in the studied wells. (a) KNW-6, (b) KW-2, (c) K-26, and (d) KSE-1X.

was primarily conducted using data obtained from well logs of five specific wells, namely, KNW-6, KW-2, K-26, K-1X, and KSE-1X. The well logs entail several types: gamma-ray logs (GR), sonic logs (DT), density logs (ROHB), neutron porosity logs (NPHI), shallow and deep resistivity logs (LLS and LLD, respectively), photoelectric factor (PEF), and spectral gamma logs (URAN, THOR, and POTA). The petrophysical properties and lithofacies of the reservoir are determined, utilizing industry standard well log analysis software.

The reservoir rock's unique lithofacies were estimated based on cross-plots of neutron density, M-N, and the matrix identification cross-plots (apparent matrix grain density- (RHOmaa-) apparent volumetric cross-section (Umaa)). Subsequently, the petrophysical characteristics were computed and graphically depicted in a vertical

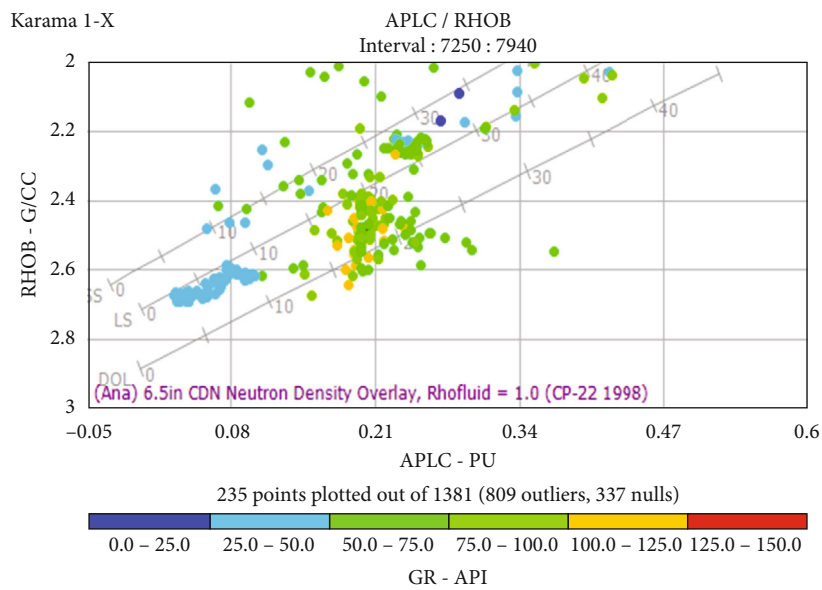

(a)

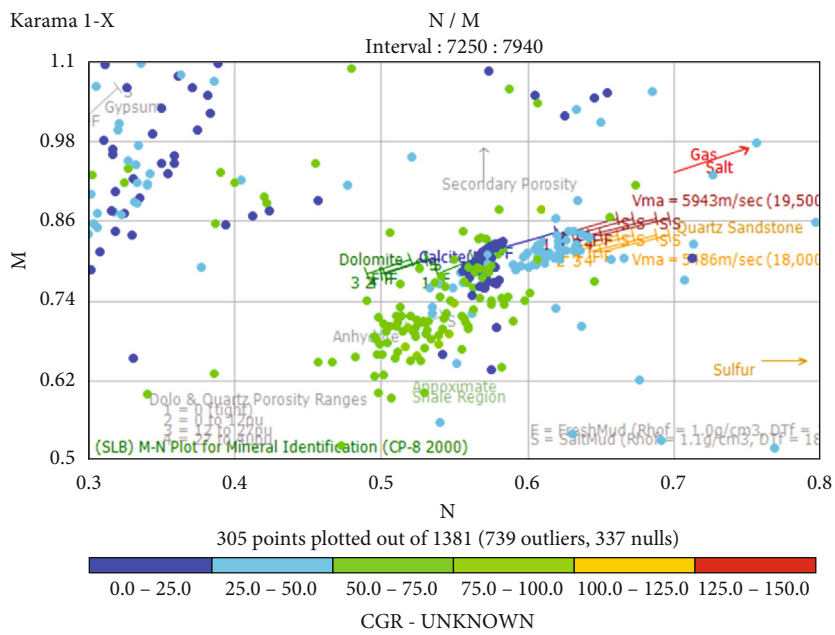

(b)

Figure 5: Continued.

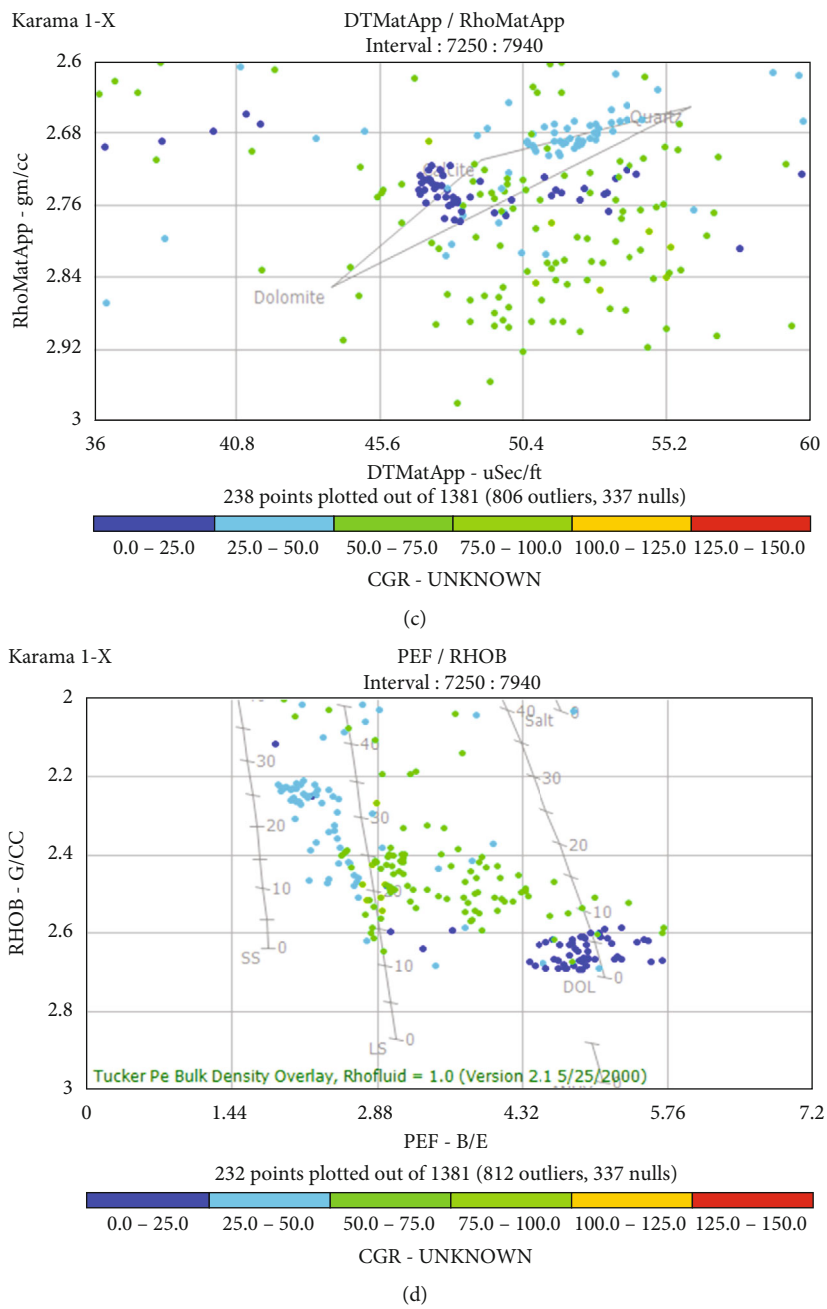

Figure 5: Lithology and mineralogy cross-plots for Karama 1-X well: (a) dolomite and limestone clustering on neutron porosity- (APLC-pu-) bulk density (RHOB); (b) calcite, anhydrite, and quartz clustering on M-N cross-plot; (c) calcite and quartz clustering confirmed with anhydrite diffused cluster; (d) dolomite and limestone clustering, possibly with low porosity calcite point (blue) plotting as dolomite.

Cross-Plot Interpretation (CPI) format, as well as in a horizontal representation utilizing isoparametric maps.

The investigation focused on the geochemical progression of upper Cretaceous source rocks within the research area, employing two unique techniques. The initial methodology employed in this study involved the utilization of Interactive Petrophysics (IP) software to conduct well log response analysis. The methodology employed in this study involved the utilization of the distinction between resistivity and sonic logs to infer the existence of a well-developed source rock [34]. The second approach focused on conducting geochemical analyses, including the determination of Total Organic Carbon (TOC) and the examination of pyrolysis analysis outcomes.

Rock-Eval pyrolysis quickly assesses rocks' thermal maturity and hydrocarbon generation potential, according to Peters [35]. The gradual heating of crushed materials in an inert environment converts bitumen to free organic compounds (bitumen) and produces pyrolytic products from insoluble organic matter (kerogen). This method is popular because it is efficient, requires few samples, and is simpler than standard extraction methods.

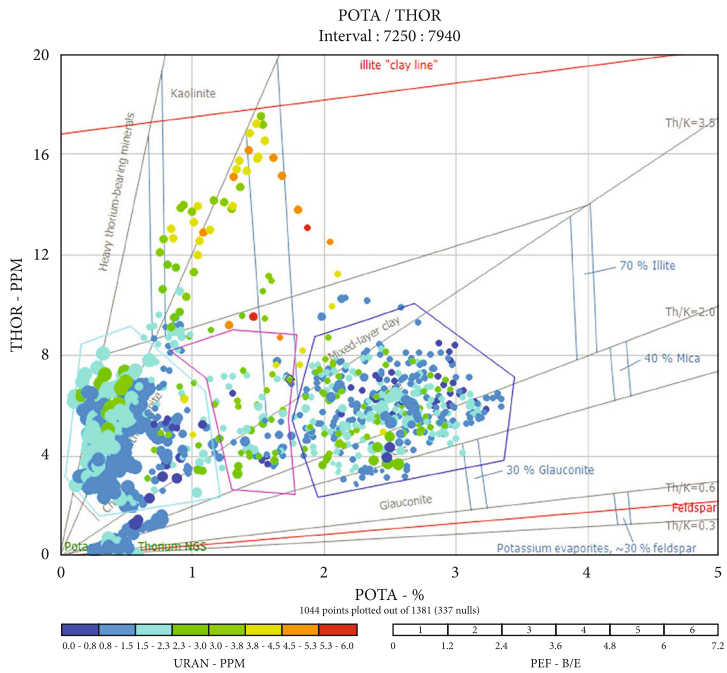

(a)

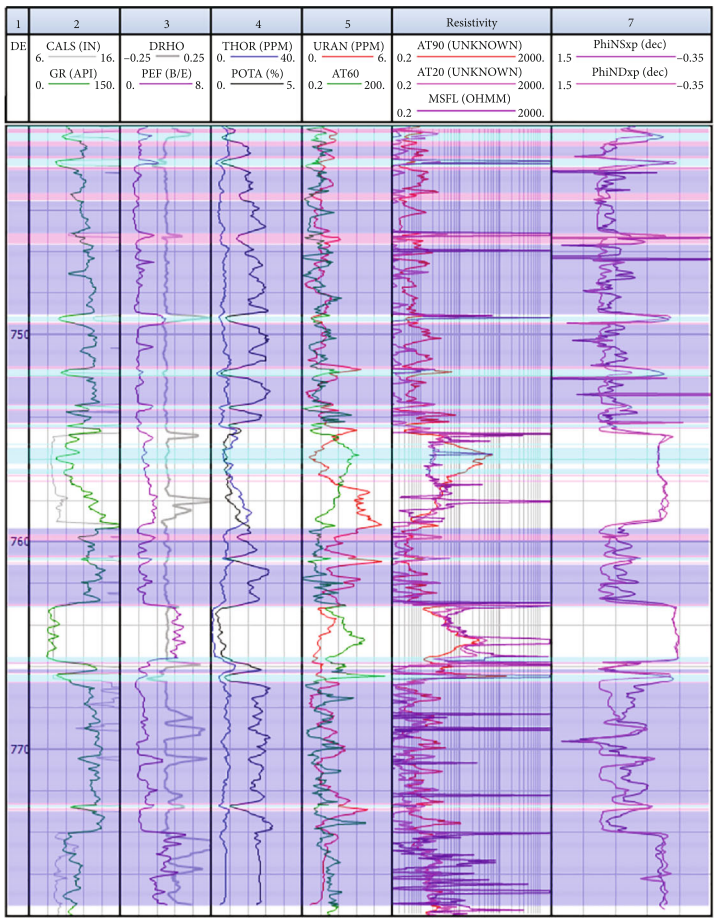

(b)

Figure 6: (a, b) Lithology PEF clustering (circle) size in thorium-potassium cross-plot with montmorillonite and illite as dominant clays; (b) vertical amalgamation of the identified clusters, indicating lithology relevance with anomalously high uranium and high-value density correction (DRHO) and PEF spikes reflecting fracture zones.

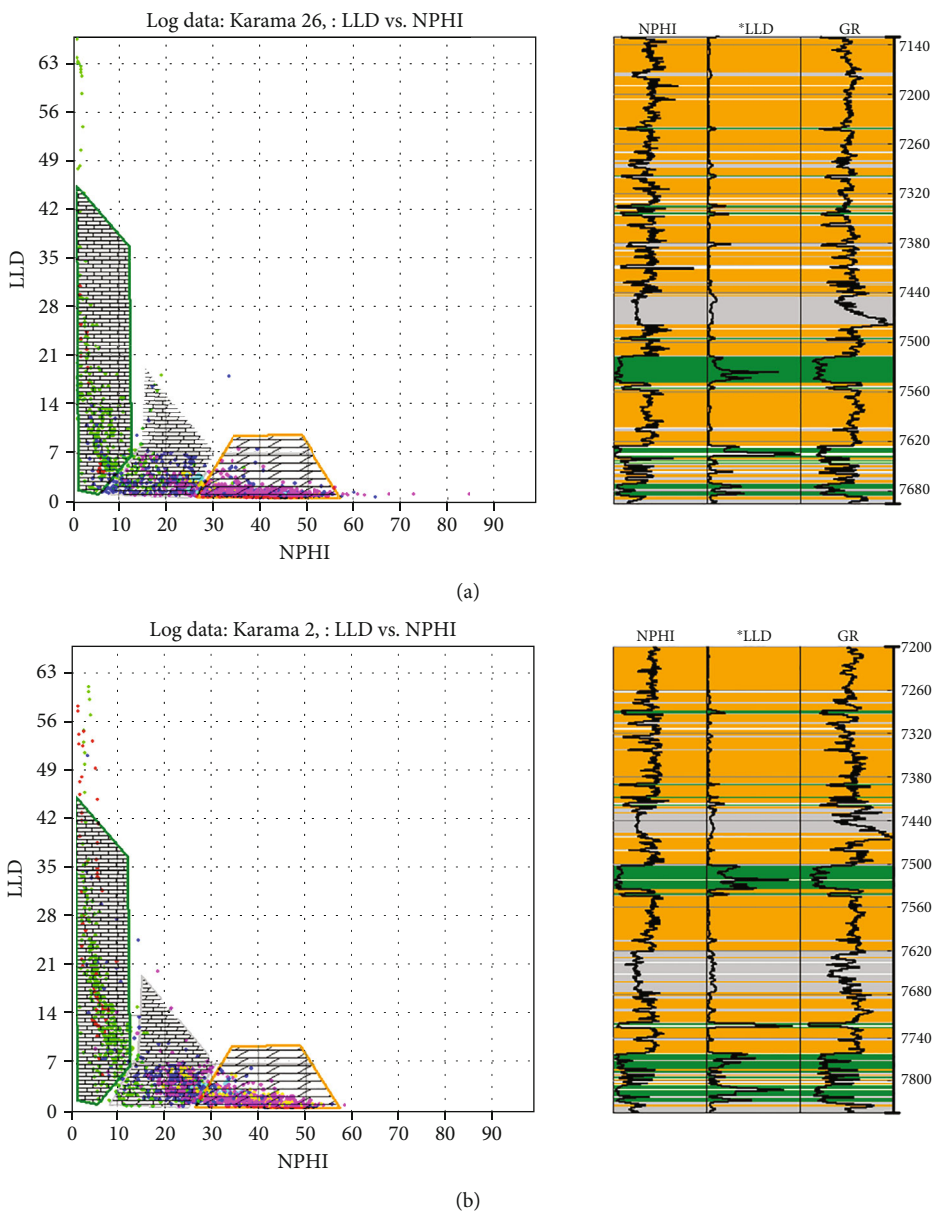

Figure 7: NPHI-LLD cross-plot with outlined log facies polygons for (a) Karama 26 and (b) Karama 2; vertical amalgamation and consistency signify lithofacies grouping.

Table 1: The petrophysical characteristics of the Abu Roash (G) reservoir in the Karama oil field.

Well no.	Reservoir	Total thickness (ft)	Net pay (ft)	Effective porosity ($Ø_{eff}$ %)	Shale volume (V_{sh} %)	Water saturation (S_w %)	Hydrocarbon saturation (S_{hr} %)
KNW-6		630	54	20	24	47	53
KW-2		283	69	22	23	44	56
K-26	AR (G)	564	107	30	13	55	45
K-1X		692	151	24	13	51	49
KSE-1X		1518	168	20	18	40	60

In the K-1X and KSW-8 wells, 27 cutting samples from Upper Cretaceous sources (AR/F, AR/G, and U. Bahariya) were studied to evaluate the source rock. These samples were mostly sandstone, limestone, and shale. LECO SC632 and Rock-Eval 6 instruments measured TOC weight percent and pyrolysis. Five samples from K-1X and six from KSW-

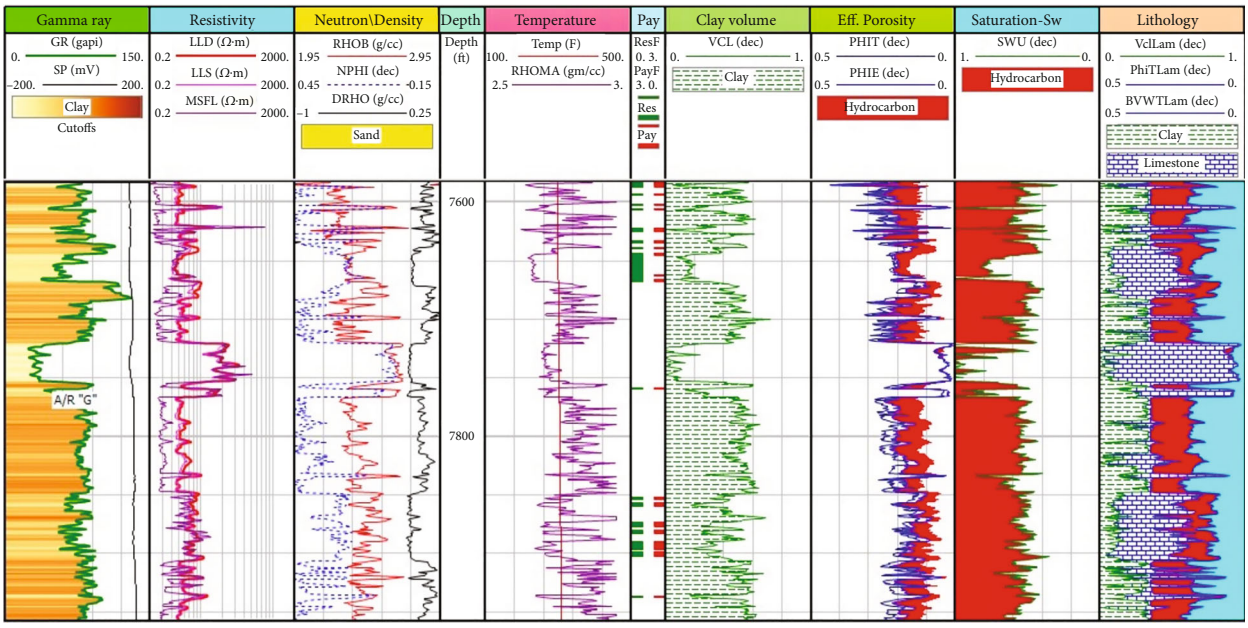

Figure 8: Vertical distribution of the petrophysical characteristics of Abu Roash (G) Member using CPI in the KNW-6 well.

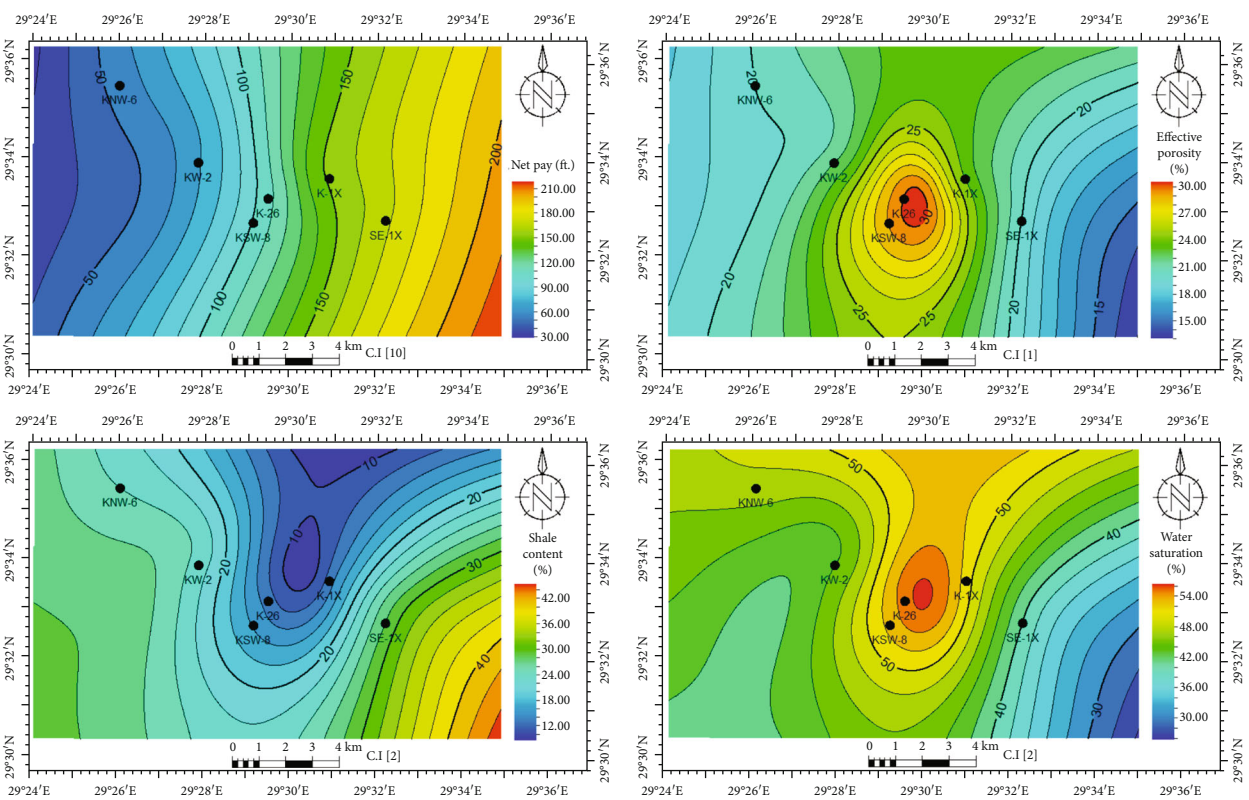

Figure 9: Horizontal distribution of the petrophysical characteristic in the AR/G reservoir through the isoparametric maps.

8 showed AR/F. Five K-1X samples represent AR/G. The K-1X well had eleven U. Bahariya Formation samples.

The Qarun Petroleum Company took cutting samples from the study area at various depths and analyzed them using geochemical pyrolysis analysis (gas type (S1, S2, or S3), Total Organic Carbon (TOC), Tmax, hydrogen index (HI), oxygen index (OI), etc.) and provided a geochemical report.

The results are simultaneously evaluated to identify source rock characteristics such as organic richness, kerogen

type, and thermal maturity, in addition to the identification of the geological environment. The data were signed and plotted on diagrams using Grapher 2015.

4. Results and Discussions

4.1. Well Log Analysis. A thorough analysis of well data was conducted in the Karama oil field, with particular emphasis on five wells located within the designated research region (Figure 1(b)). The main aim of this study was to provide a detailed and accurate description of the petrophysical properties associated with the reservoir layer referred to as Abu Roash G Member. The reservoir's formation water resistivity value (Rw) was measured within the range of 0.0123 to 0.0489 ohm\m. Subsequently, the prescribed threshold values for the Abu El Gharadig Basin were implemented, encompassing an effective porosity of 9%, a saturation level of 65%, and a shale content of up to 35% [7, 9, 27].

The determination of lithological characteristics in reservoir rocks holds significant importance in the field of petroleum exploration and production. The process entails the identification and analysis of the constituent elements and properties of the geological formations inside a reservoir, hence facilitating the comprehension of the reservoir's capacity for hydrocarbon extraction. The interpretation of neutron porosity and density cross-plots is a commonly employed technique for lithological identification. Neutron porosity–density cross-plots are utilized by geoscientists to distinguish between different lithologies found in the reservoir, ascertain the porosity of the reservoir rocks, and aid in the assessment of fluid saturation within the reservoir [36–39].

From the neutron porosity–density cross-plots (Figure 4) of the Abu Roash G reservoir in the study area, it is observed that the majority of the plotted points are scattered very close to the dolomite line, especially for neutron porosity greater than 20%. Less than 15% of the points coincide with or in the vicinity of the limestone trend. Effective porosity is ranging from 7 to 27% in the KNW-6 well, and density is ranging from 2.1 to 2.7 g/cm^3. In the KW-2 well, the effective porosity is ranging from 8 to 35%, and density is ranging from 2.1 to 2.7 g/cm^3. In the K-26 well, the effective porosity is ranging from 10 to 30%, and density is ranging from 1.85 to 2.7 g/cm^3. In the K-1X well, the effective porosity is ranging from 5 to 27%, and density is ranging from 2.1 to 2.5 g/cm^3. This indicates that the reservoir lithology is mainly composed of about 85% dolomite. Dolomitization reflects the porosity-enhancing diagenetic history of the carbonate reservoir of this field.

M-N cross-plots, commonly referred to as Pickett plots, are extensively utilized in the field of petrophysics for the purpose of interpreting reservoir rocks. The plots in question pertain to the graphical representation of the ratio between resistivity log measurements (M) and porosity readings (N), with the y-axis representing the former and the x-axis representing the latter. The analysis of M-N cross-plots offers significant insights into the lithology, fluid saturation, and rock characteristics of the reservoir [36, 39].

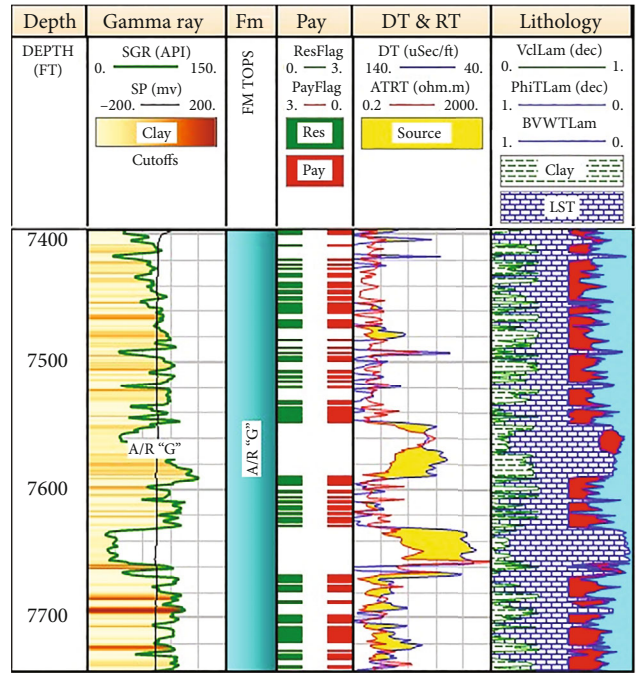

Figure 10: Electric well logs of the studied successions in the K-1X well, Abu El Gharadig Basin.

M-N cross-plots are utilized as means of discerning various lithologies present inside a reservoir. Various rock types have distinct responses on cross-plots as a result of changes in mineral composition, pore structure, porosity, and fluid content. Through the examination of data point positions on the plot and the consideration of lithology-specific patterns, geoscientists are able to deduce the prevailing lithology or lithologies that exist inside the reservoir [37, 38]. Matrix mineral methods such as RHOmaa-Umaa cross-plotting offer porosity-independent mineralogy [40]. RHOmaa-Umaa cross-plotting is more reliable than other log response analysis methods [41].

Lithology and mineralogy cross-plots, of neutron porosity versus bulk density (Figures 4(a)–4(d) and Figure 5(a)), and M versus N; DTMApp (apparent matrix transit time) versus RHOmaa (apparent matrix grain density); and Bulk density versus photoelectric factor (PEF) (Figures 5(b)–5(d)) reflect the dominant lithotypes of limestone, dolomitic limestone, sandstone, and dolomite, with considerable proportion of anhydrite. The complex mineralogy of the Abu Roash G reservoir at the K-1X well of the Karama oil field is evident and needs to be integrated in the reservoir geomodel of four or three lithotypes. Most data points are distributed around the region between the calcite and dolomite regions, with a few data points in proximity to the quartz region. The observed geological characteristics may suggest the existence of limestone reservoirs, as well as the presence of shale formations interspersed with occasional sandstone layers. The upward scattering of certain dots is attributed to secondary porosity or the effects of anhydrite or gypsum. The computed gamma ray color scale is used to evaluate the consistency of clustering from one cross-plot to another; it is noteworthy that PEF versus RHOB manifests a

Table 2: The pyrolysis analysis data for the available source rock formations in the Karama oil field.

Well name	Formation	Depth	TOC[1]	S1[2]	S2[3]	S3[4]	S1 + S2	Tmax[5]	HI[6]	OI[7]	PI[8]
K-1X	AR/F	7150	1.54	0.63	4.32	1.5	4.95	428	281	97	0.13
		7170	2.8	1.02	21.4	0.91	22.42	421	764	33	0.05
		7180	2.95	1.21	23.85	0.74	25.06	422	808	25	0.05
		7230	3.6	1.62	32.87	0.75	34.49	421	913	21	0.05
		7250	1.47	0.2	4.23	0.8	4.43	430	288	54	0.05
	AR/G	7300	0.64	0.27	0.77	0.76	1.04	429	120	119	0.26
		7350	0.52	0.12	0.75	0.57	0.87	376	144	110	0.14
		7400	0.72	0.25	1.99	1.22	2.24	432	276	169	0.11
		7450	0.64	0.25	1.91	0.5	2.16	429	298	78	0.12
		7550	0.8	0.28	1.65	0.49	1.93	431	206	61	0.15
	U. Bahariya	7720	0.64	0.44	1.69	1.41	2.13	419	264	220	0.21
		7750	0.48	0.16	0.92	0.3	1.08	391	192	63	0.15
		7780	0.62	0.2	1.19	0.4	1.39	434	19	65	0.14
		7850	0.7	0.17	1.34	0.39	1.51	433	19	56	0.11
		8000	0.62	0.17	1	0.43	1.17	432	161	69	0.15
		8050	0.66	0.23	1.35	0.8	1.58	435	205	121	0.15
		8150	0.55	0.15	0.74	0.53	0.89	382	135	96	0.17
		8350	0.63	0.18	1.24	0.99	1.42	381	197	157	0.13
		8400	0.98	0.22	1.57	0.8	1.79	430	160	82	0.12
		8550	0.8	0.25	1.84	0.71	2.09	432	230	89	0.12
		8600	0.67	0.18	1.31	0.63	1.49	383	196	94	0.12
KSW-8	AR/F	7040	5.84	21.21	0.22	425	27.05	442	—	—	—
		7050	1.47	15.42	0.11	426	15.89	431	—	—	—
		7055	1.43	14.26	0.07	427	14.69	436	—	—	—
		7060	3.93	16.56	0.15	426	20.49	441	766	55	—
		7065	1.32	11.94	0.11	424	12.26	433	589	43	—
		7070	2.29	11.74	0.22	426	12.03	435	—	—	—

[1]Total Organic Carbon (weight percent of the whole rock). [2]Low hydrocarbon yield (mg hydrocarbon/g rock). [3]High hydrocarbon yield (mg hydrocarbon/g rock). [4]Organic carbon dioxide yield (mg hydrocarbon/g rock). [5]Temperature at which maximum emission of high-temperature (S2) hydrocarbon occurs (deg.C.). [6]Hydrogen index (mg hydrocarbon/g TOC). [7]Oxygen index (mg CO_2/g TOC). [8]Production index ($S1/S1 + S2$).

significant cluster around the dolomite trend that is mapping around the calcite on M-N and DTMApp-RHOmaa cross-plots. The thorium- (THOR-) potassium (POTA) cross-plot (Figure 6(a)) with color scale of uranium (URAN) and circle size scale for PEF reflects the montmorillonite, illite, kaolinite, and mica clay mineralogy of AR-G. The thorium-potassium clustering of the mineralogical grouping as evidenced by the coinciding PEF circle-size clustering is characterized by vertical amalgamation (Figure 6(b)). Interpreted fractures are represented by narrow zones of uranium and PEF highs or spikes correlating with spikes in bulk density correction (DRHO) (Figure 6(b)). The narrow zones of uranium "highs" are likely correlating with fractures or erosional services; also, Uranium highs can correlate with hydrocarbon-source organic richness [42, 43]. The well log facies three polygons (low, medium, and high porosity) (Figures 7(a) and 7(b)) on the NHPI-LLD log cross-plot for Karama 26 and Karama 2 manifests vertical amalgamation that signifies lithofacies consistency; argillaceous limestone/anhydrite (green), limestone and dolomitic limestone (grey), and dolomite (gold).

Following the determination of the rock facies type and the calculation of petrophysical properties within the reservoir, the findings were vertically depicted to showcase the vertical variations in both the rock facies and the properties across the study wells located in the Karama field. Additionally, a series of petrophysical maps were constructed to visually represent the horizontal variations in the properties, thereby facilitating an understanding of their lateral changes.

The depths observed in the study wells varied from 6334 feet in the KSE-1X well, 7200 feet in the KW-2 well, 7400 feet in the K-1X well, 7551 feet in the KNW-6 well, and 7137 feet in the K-26 well. Regarding the petrophysical qualities of the reservoir layer, the AR-G reservoir properties can be summarized as follows: The net pay thickness of the reservoir layer varied from 54 feet in the KNW-6 well to 168 feet in the KSE-1X well. Additionally, the effective porosity values ranged from 20% in KNW-6 and KSE-1X to 30% in the K-26 well. The shale content within the research region exhibited an approximate value of 24% in the KNW-6 well. The water saturation levels in KSE-1X and K-26 wells varied between 40% and 55%, respectively. Consequently, the

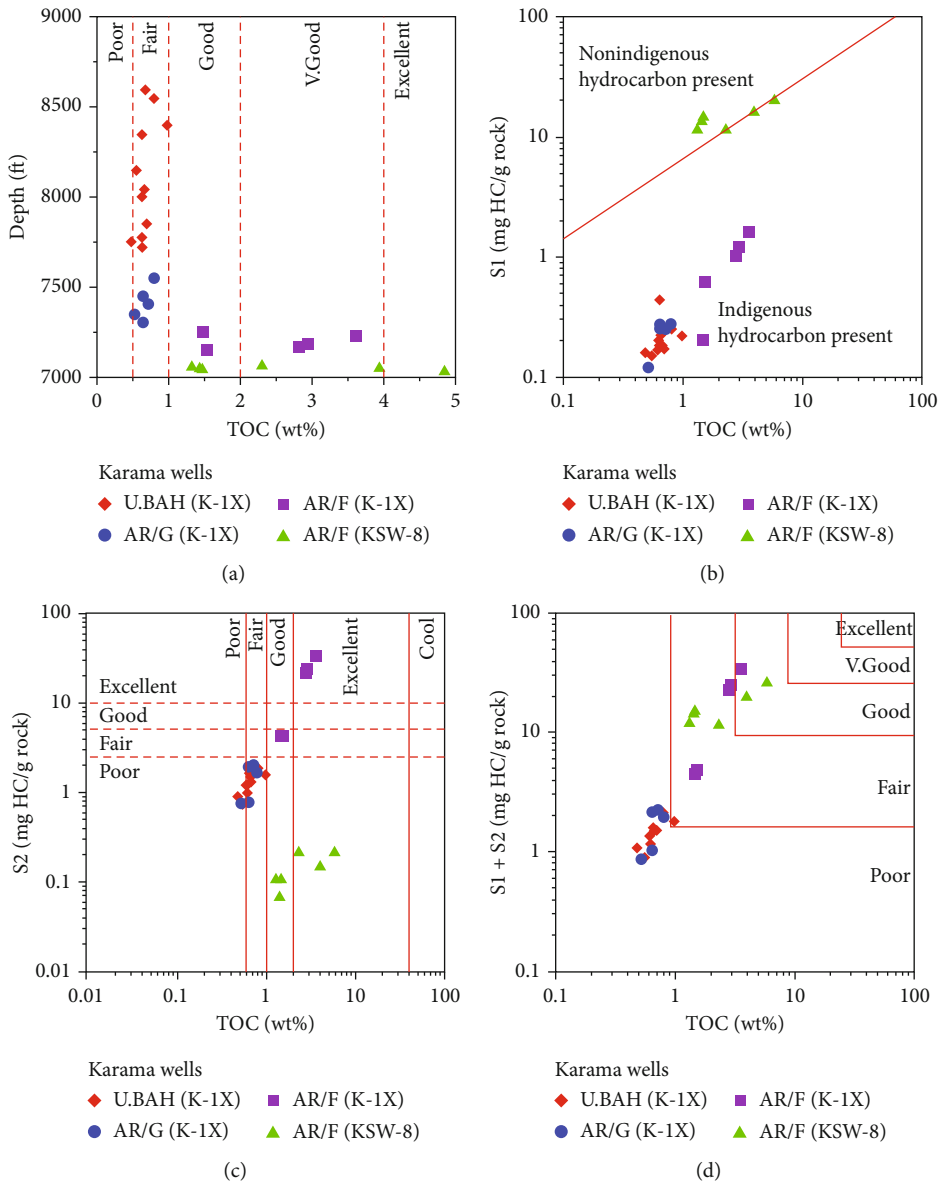

Figure 11: (a) The relations between the TOC and depth after Peters and Cassa [50]; (b) the relation between the TOC and S1 according to Hunt [62]; (c) the relation between the TOC and S2 according to Dembicki [63]; (d) the relation between the TOC and S1 + S2 according to Dembicki [63] illustrating the organic richness of the selected 27 samples in the K-1X and KSW-8 wells in the Abu El Gharadig Basin.

saturation percentage of hydrocarbons might potentially exceed 60%, as seen in Table 1.

Figure 8 depicts the Computer Processed Interpretation (CPI) study conducted on the KNW-6 well, serving as an instructive example. This study covers ten discrete pathways, commencing with the gamma ray pathway and ends with the lithofacies pathway. The results of this investigation suggest that the rock facies identified in the AR/G, at this well, consists predominantly of limestone and shale, with occasional instances of sandstone interbeds. The presence of vertical facies variation is apparent, as indicated by the prevalence of limestone facies in the middle and lower zones, progressively decreasing in abundance as we move downwards. This transition is accompanied by the emergence of shale facies interspersed with sandstone.

Figure 9 illustrates the spatial distribution of outcomes seen in the several petrophysical maps. The net pay thickness distribution map reveals that there is an increase in reservoir thickness in the middle and eastern regions of the research area, with the highest thickness measuring approximately 168 feet in the KSE-1X well. The effective porosity distribution map reveals an augmentation in the central and western regions. Conversely, the clay content exhibits an escalation towards the central direction, while demonstrating a noticeable decline in the northern portion of the investigated area. Ultimately, the distribution map illustrating the saturation of the Abu Roash G reservoir with hydrocarbons in the Karama field revealed an upward trend in the central and northern regions. This pattern coincides with the rise in thickness and effective porosity, as well as the decline in shale content.

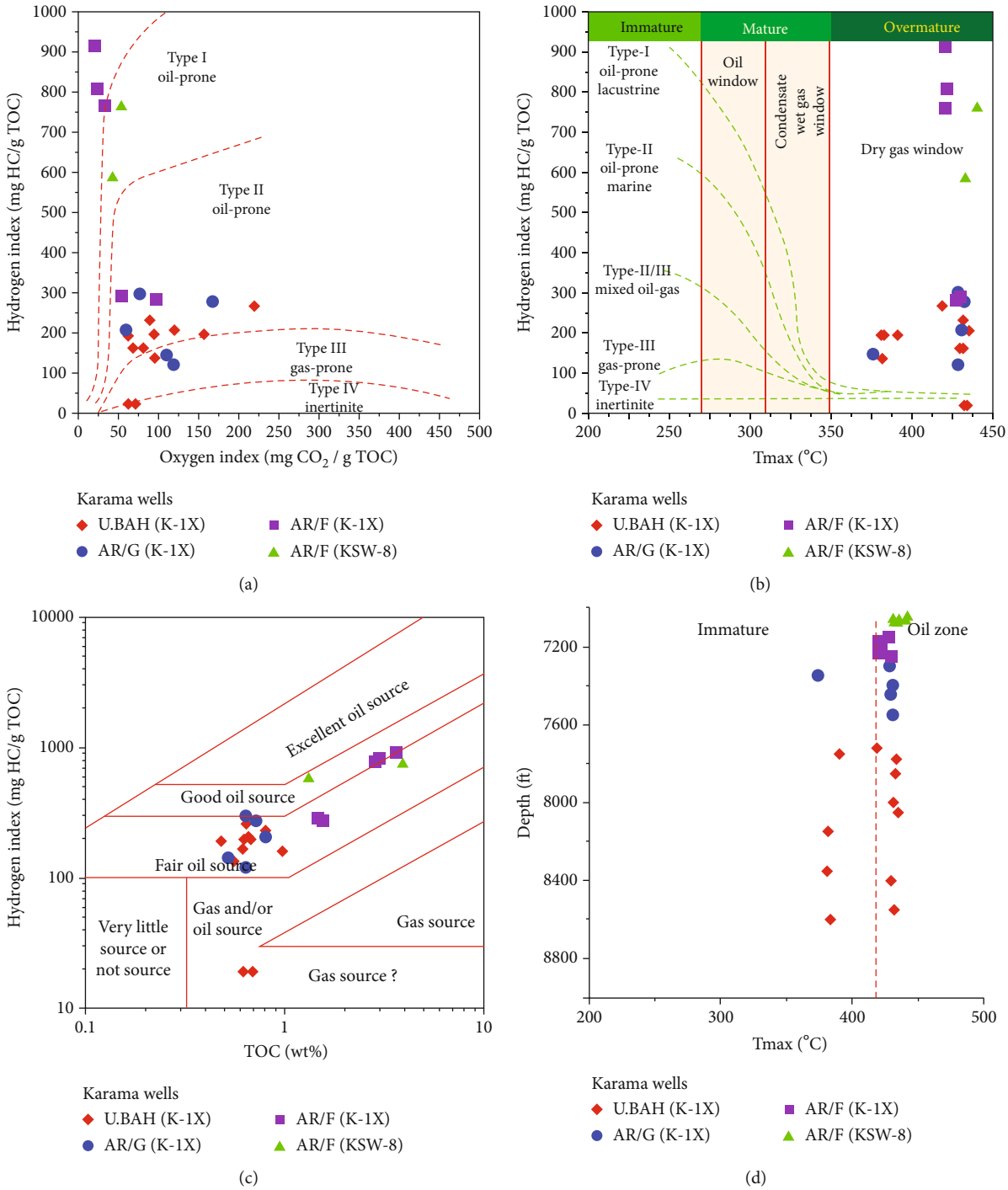

Figure 12: (a) Adapted Van Krevelen diagram based on Espitalie et al.'s work in 1977 [53], illustrating kerogen type in the K-1X and KSW-8 wells. (b) Correlation between Tmax and HI, as per Espitalie et al.'s research from 1985 [22]. (c) Characterization of source rocks using a plot of HI versus TOC, following Jackson et al.'s methodology from 1985 [64]. (d) Relationship between Tmax and depth, providing insights into the immature and oil zones.

The findings suggest that the Abu Roash G Member holds significant importance as a reservoir in the study area. It is noteworthy that the properties of this reservoir are influenced by the structural conditions of the Abu El Gharadig Basin area in the northern Western Desert, as discussed by Reda et al. [10] and Mamdouh et al. [9].

4.2. Well Log Response. According to Passey et al. [34], the utilization of acoustic and resistivity logs plays a crucial role in identifying the existence of diverse source rock formations within a geological framework. The utilization of a log-based methodology has played a crucial role in comprehending the intricate geological characteristics of sedimentary basins.

The resistivity values exhibit notable changes, particularly with regard to the higher values, which have important implications suggesting the existence of well-developed, productive source rock formations [44]. The analysis and understanding of these logs are contingent upon the level of thermal maturity, providing valuable insights into the various phases of hydrocarbon formation. On the other hand, there is a correlation between low resistivity values and the presence of oil-source rocks that are either immature or overmature. In such cases, it is likely that hydrocarbons have been evacuated from these rocks [45]. Within the framework of the K-1X well, the correlation between resistivity and acoustic logs provides significant insights into the characteristics of source rock formations (Figure 8).

The K-1X well, which has been a significant focus of research, encountered the AR/G Member (Upper Cretaceous) at a depth of 7400 feet, with a thickness of around 629 feet. The unique electrofacies (Figure 10) of this deposit are characterized by an increase in sonic values (DT) ranging from 51 to 115 μs/ft, accompanied by an elevation in resistivity values (RT) ranging from 0.298 to 1950 ohm/m. The electrofacies exhibit distinctive features that are indicative of the presence of organic-rich sedimentary layers. These characteristics are significant as they suggest that the AR/G formation has the potential to function as a source rock, in addition to being the primary reservoir in the Karama oil field.

4.3. Source Rock Evaluation

4.3.1. Organic Richness. Several notable researchers [10, 14, 44, 46–51] have collectively underscored that the evaluation of source rocks is fundamentally indicated by three crucial factors: organic abundance, kerogen classification, and the thermal maturity of organic material.

Table 2 presents a complete summary of the examination of pyrolysis data for specific source rocks found in the Karama oil field. The analysis was performed on a total of twenty-seven samples of shale cuttings derived from the K-1X and KSW-8 wells. These samples encompassed various formations, including the AR/F and AR/G Members of the Abu Roash Formation, as well as the Upper Bahariya Formation. The AR/F Member exemplifies a diverse assemblage of shale and sandstones, which are interspersed with layers of limestone and siltstones. The organic matter abundance present in this geological formation is evaluated based on the analysis of eleven samples (Figures 11(a)–11(d)). These samples consist of five samples obtained from the K-1X well and six samples obtained from the KSW-8 well. The Total Organic Carbon (TOC) content of these samples ranges from 1.32 to 5.84 weight percent. The depicted range illustrates a continuum of organic richness, spanning from good to excellent levels (Figures 11(a)–11(d)). The AR/G Member predominantly comprises limestone and shale, with intermittent deposits of siltstones and sandstones. Finally, it should be noted that the Upper Bahariya Formation is primarily composed of argillaceous sandstone. The geological formation under investigation demonstrates the presence of organic matter abundance, as indicated by the examination of five samples in AR/G and eleven samples from the Upper Bahariya, which were acquired from the K-1X well. The samples exhibit a variety of Total Organic Carbon (TOC) content, with values ranging from 0.52 to 0.72 and 0.48 to 0.98 weight percent. These values indicate a state of fair organic richness (Figures 11(a)–11(d)).

Table 3: The available biomarker data for the studied source rock formations in the Karama oil field.

Well name	Formation	Depth	Ph[1]/n-C18	Pr[2]/n-C17	Pr/Ph
K-1X	AR/F	7230	2.13	0.97	1.15
	AR/G	7550	0.04	0.12	2.99
	U.BAH	7720	0.82	0.75	1.04
KSW-8	AR/F	7045	0.07	0.12	1.32
		7050	0.23	0.36	1.38
		7060	0.06	0.11	1.51
		7070	0.13	0.24	1.52

[1]Phytane. [2]Pristane.

Interestingly, apart from three samples obtained from the AR/F Member in the KSW-8 well, all the chosen samples demonstrate a connection with the existence of native hydrocarbons. This is apparent from the association observed between Total Organic Carbon (TOC) and the level of free hydrocarbons (S1) (Figure 11(b)).

Upon further examination of the data, it becomes evident that there is a correlation between Total Organic Carbon (TOC) and pyrolysis-derived parameters, specifically S2 (representing hydrocarbon potential) and S1 + S2 (representing the overall hydrocarbon generation potential) (Figures 11(b) and 11(c). This observation provides additional valuable information and a deeper understanding of the subject matter. Within the context of the AR/F Member, the values of the producing source potential (S1) exhibit a range spanning from 0.2 to 21.21 mgHC/g. This wide spectrum of values indicates a continuum that encompasses organic source potential ranging from good to excellent.

The AR/G Member demonstrates S1 values ranging from 0.12 to 0.28 mgHC/g, suggesting a poor to fair organic source potential. The Upper Bahariya Formation exhibits the same pattern, with S1 values ranging from 0.15 to 0.44 mgHC/g rock, indicating a state of poor to fair organic source potential.

Upon further investigation, it has been shown that the three sources under consideration exhibit a range of producing source potential values. For the AR/F Member, these values range from 0.07 to 32.87 mgHC/g. Similarly, the AR/G Member has potential values ranging from 0.75 to 1.99 mgHC/g. Lastly, the Upper Bahariya Formation exhibits potential values ranging from 0.74 to 1.84 mgHC/g. These formations collectively exhibit a spectrum of organic source potential ranging from poor to outstanding.

4.3.2. Kerogen Type and Maturation. Waples [51] classified organic materials using the hydrogen index (HI) and made a substantial contribution. Based on this idea, Peters [35], Peters and Cassa [50], Baskin [52], and Carvajal-Ortiz and Gentzis [46] have further supported the relationship

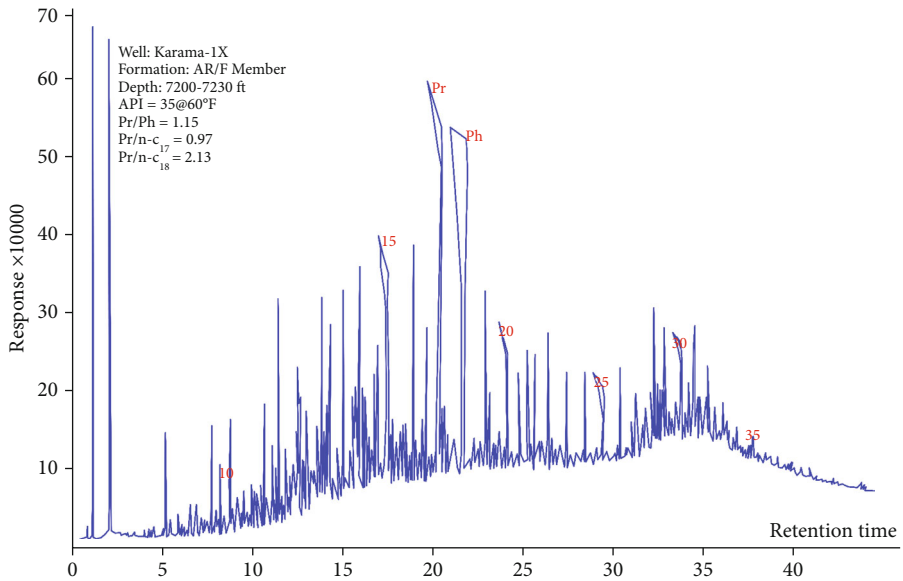

Figure 13: The Gas Chromatogram (GC) displaying the C_{4+} saturated hydrocarbons found in the AR/F source rock member within the K-1X well.

between hydrogen index (HI) values and kerogen classifications, providing a framework for source rock evaluation. Type III kerogen, which is a natural gas generative, has hydrogen index (HI) values of 50 to 200 mgHC/g TOC. Values of 200–300 mgHC/g TOC indicate type II/III kerogen, which is typically indicative of gas and oil generation. Type II kerogen, which produces oil and gas, has values of 300 to 600 mgHC/g TOC [14, 35, 46, 50, 52].

The observed AR/F, HI, and OI values ranging from 281 to 913 mg/g and 21 to 97 mg/g, respectively, evidence type I and II kerogen (Figure 12(a)). The link can be seen using a modified Van Krevelen diagram, as elucidated by Espitalie et al. [53]. In a similar vein, the AR/G Member has HI and OI values that span a range of 120 to 298 mg/g and 61 to 169 mg/g, respectively, which suggests the presence of both type II and type III kerogen (Figure 12(a)). The HI and OI values observed in the Upper Bahariya Formation exhibit a range of 19 to 264 mg/g and 63 to 220 mg/g, respectively, which suggests the presence of type II and III kerogen (refer to Table 2 and Figure 12(a)).

To assess the level of maturity of petroleum source rocks, various metrics are considered, including Vitrinite Reflectance (Ro), oxygen index (OI), production index (PI), and the temperature at which the kerogen reaches its peak hydrocarbon generation (Tmax). The maturity assessment additionally offers valuable insights into the hydrocarbon generation capacity of source rocks. Within the framework of this investigation, it is shown that the AR/G Member and Upper Bahariya Formation can be considered as fair sources of oil, but most of the samples from the AR/F Member demonstrate attributes indicative of good oil sources (Figures 12(b)–12(d)).

The notion of maturity is additionally encompassed by Tmax values, which function as indicators for the thermal maturity of source rocks. The analysis indicates that the AR/F Member is located inside the mature oil zone, while the AR/G Member and Upper Bahariya Formation are found in both the mature and immature zones.

4.4. GC Biomarker Analysis

4.4.1. C15+ Normal Alkanes. The investigation of extracted samples, which were subjected to Gas Chromatography (GC) analysis, involved the quantification of n-alkanes and the isoprenoids pristane (Pr) and phytane (Ph), as detailed in Table 3. The GC of the AR/F and AR/G source rock members from the Upper Cretaceous period is clearly depicted in Figures 13 and 14, respectively.

The GC signature of the AR/F Member exhibits distinct peaks that extend from n-C4 to n-C41 (Figure 13), indicating the presence of type I and II kerogen. The isoprenoid Pr/Ph ratio exhibits a value of approximately 1.15, while the Pr/n-C17 values demonstrate a value of 0.97, and the Ph/n-C18 values indicate a value of 2.13 (Table 3 and Figure 15). The observed range of composition in this study is indicative of a marine organic matter with contribution of a biodegradation stage. This suggests the presence of a reducing environment characterized by type I and type II kerogen (Figure 15(a)), which have the capacity to generate oil [54–56].

For the extracted sample of the AR/G Member, the major peaks span n-C2 to n-C41 (Figure 14), a clear evidence of type II kerogen. Notably, the isoprenoid Pr/Ph ratio is recorded as 2.99, and the Pr/n-C17 value is 0.12 (Table 3). In comparison, the Ph/n-C18 ratio stands at 0.04. These properties hint to a marine organic source, under a more reducing condition. This composition coincides with type II kerogen, largely oil-prone in nature.

5. Discussion and Conclusions

This study is aimed at analyzing the reservoir rocks and source rocks in the Karama oil field and evaluating their qualities. The authors utilized a dataset from five wells that included important recordings for studying the Abu Roash G Member, which is the main reservoir in the area. They

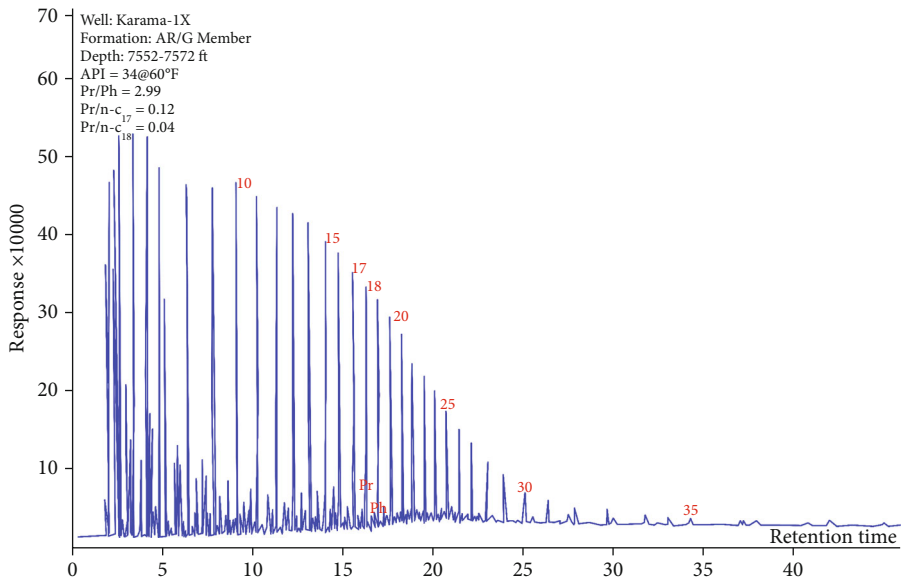

Figure 14: The Gas Chromatogram (GC) displaying the C_{4+} saturated hydrocarbons found in the AR/G source rock member within the K-1X well.

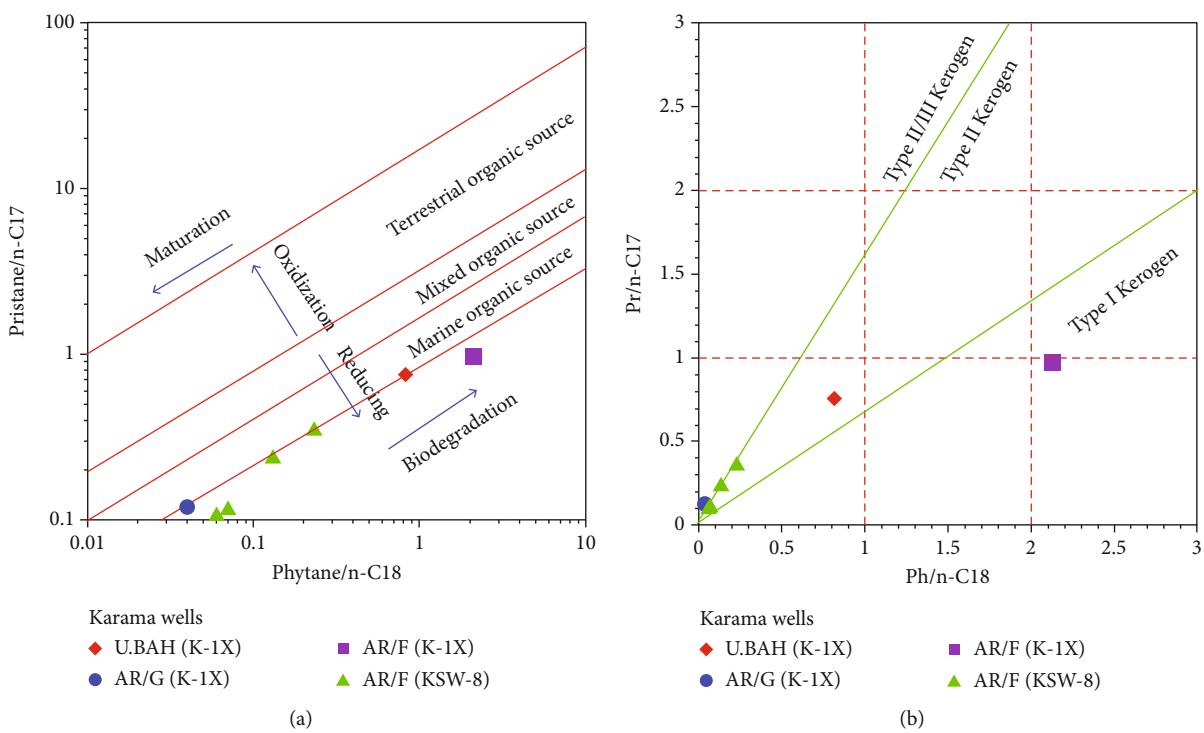

Figure 15: (a) Pr/n-C17 versus Ph/n-C18 cross-plot for the GC markers in the Abu El Gharadig Basin, adapted from the work of [65]. (b) Cross-plot illustrating Pr/n-C17 versus Ph/n-C18, following the approach of [66].

also included data from one additional well for geochemical analysis and pyrolysis studies to assess the source rocks.

From a petrophysical perspective, the classification of the Abu Roash G Member as a basic reservoir is supported by the favorable outcomes of the petrophysical property analysis. These findings reveal that the thickness of the reservoir in the Karama field measures 168 feet and exhibits an increasing trend towards the east and north directions. Additionally, the effective porosity ratio of 30% is concentrated in the central area of the region, presenting a notable contrast. Consequently, there is a notable decline in the proportion of clay content in the central and northern regions. Additionally, towards the conclusion, there is an observed increase in the level of water saturation (55%), particularly in the central and northern areas. Furthermore, it has been observed that the ratios and values are significantly

influenced by variations in the composition and the alteration of rock facies, occurring both in the vertical and horizontal dimensions. Hence, the study suggests exercising prudence during the drilling of new development wells, particularly because the optimal locations are situated in the eastern region of the study area.

Three rocks, namely, Abu Roash F and G Members and the Upper Bahariya Formation, were analyzed from a geochemical perspective as prospective reservoir rocks in the region that supplies the reservoir layer. The Abu Roash F Member is distinguished by a substantial proportion of organic matter, ranging from 1.32 to 5.84. This high organic content indicates a significant abundance of organic richness, making it an excellent source of this valuable resource. On the other hand, the AR/G Member and U. Bahariya Formation have a relatively low organic matter content and are categorized as fair in quality. Regarding the kerogen classification, the source rocks associated with the Abu Roash F Member can be categorized within the type I and type II kerogen, indicating a significant potential for oil generation. The Abu Roash G Member and Upper Bahariya Formation are situated within the type II and III kerogen spectrum, hence enabling the generation of oil or gas. Based on the findings derived from the analysis of the GC biomarker data, it can be inferred that the prevailing environment in the research area is predominantly characterized by a maritime setting, with environmental conditions exhibiting a tendency towards reduction throughout most of the samples employed in the study.

In conclusion, the region encompasses a single reservoir and three distinct source rocks. Empirical evidence has substantiated the great efficacy of utilizing tanks for oil extraction in the Karama field. The Abu Roash F Member has been identified as the most prominent source rock based on empirical evidence. Consequently, it is widely assumed to serve as the principal source rock for the Abu Roash G reservoir. It is worth noting that both the Abu Roash G Member and the Upper Bahariya Formation exhibit favorable geochemical characteristics.

Data Availability

The data that support the findings of this study is available from the corresponding author, upon reasonable request.

Disclosure

The funding provided by the Researchers Supporting Project, King Saud University, Riyadh, Saudi Arabia, is a non-commercial funding, and the funder provided it in support of the project without any provisions that could constitute a conflict of interest affecting the objectivity or neutrality of the manuscript.

Conflicts of Interest

We declare that we have no significant competing financial, professional, or personal interests that might have influenced the performance or presentation of the research described in the manuscript.

Acknowledgments

This research was supported and funded by the Researchers Supporting Project (Project No. RSPD2024R781) and King Saud University, Riyadh, Saudi Arabia. The authors are especially grateful to the Egyptian General Petroleum Corporation (EGPC) for providing data to its technical staff for a fruitful professional discussion and to the Qarun Petroleum Company for providing the data needed to complete this work. The publication of this article was financed with partial support from Kansas State University Open Access Publishing Fund (KOAPF).

References

[1] M. A. Abd Elhady, M. Fathy, T. Hamed, and M. Reda, "Petroleum evaluation through subsurface and petrophysical studies of Hammam Faraun Member of Belayim Formation, Bakr oil field, Gulf of Suez, Egypt," *Nature and Science*, vol. 13, no. 4, pp. 59–78, 2015.

[2] J. M. Ajdukiewicz and R. H. Lander, "Sandstone reservoir quality prediction: the state of the art," *AAPG Bulletin*, vol. 94, no. 8, pp. 1083–1091, 2010.

[3] A. R. Al Shammari, "Importance of reservoir geology and petrophysics in development and production," *Journal of Petroleum Exploration and Production Technology*, vol. 2, no. 3, pp. 271–279, 2012.

[4] A. Bakr, M. Reda, and M. Fathy, "Application of 3D static modelling and reservoir characterisation for optimal field development: a case study from the Kharita Formation, Karam field, Western Desert, Egypt," *First Break*, vol. 41, no. 11, pp. 43–51, 2023.

[5] M. K. Barakat, A. Azab, and N. Michael, "Reservoir characterization using the seismic reflection data: Bahariya Formation as a case study Shushan Basin, North Western Desert, Egypt," *Journal of Petroleum and Mining Engineering*, vol. 24, no. 1, pp. 5–15, 2022.

[6] M. H. Bekhiet, E. K. El-Sawy, H. E. El-Fouly, M. Fathy, and R. Khalil, "Subsurface structural and petrophysical study on Karama field, East Bahariya Concession, Western Desert, Egypt," *Al-Azhar Bulletin Of Science*, vol. 22, no. 2-D, pp. 61–79, 2011.

[7] T. R. El-Qalamoshy, M. I. Abdel-Fattah, M. Reda, T. H. Abdelhafeez, S. S. S. Azzam, and M. Mosaad, "A multi-disciplinary approach for trap identification in the Southern Meleiha Area, North Western Desert, Egypt: integrating seismic, well log, and fault seal analysis," *Geomechanics and Geophysics for Geo-Energy and Geo-Resources*, vol. 9, no. 1, p. 157, 2023.

[8] E. A. Gawad, M. Fathy, M. Reda, and H. Ewida, "Petroleum geology: 3D reservoir modelling in the Central Gulf of Suez, Egypt, to estimate the hydrocarbon possibility via petrophysical analysis and seismic data interpretation," *Geological Journal*, vol. 56, no. 10, pp. 5329–5342, 2021.

[9] M. Mamdouh, M. Reda, M. Z. E. Din, and T. H. Abdelhafeez, "3D petroleum reservoir modelling using seismic and well-log data to assess hydrocarbon potential in Abu Roash (G) Member, Karama oil field, North-Western Desert, Egypt," *Geological Journal*, vol. 59, no. 1, pp. 313–324, 2024.

[10] M. Reda, M. Fathy, and E. A. Gawad, "Comprehensive 3D reservoir modelling and basin analysis: an insight into petroleum geology to re-evaluate the hydrocarbon possibilities in the Siwa Basin, North-Western Desert, Egypt," *Geological Journal*, vol. 57, no. 4, pp. 1600–1616, 2022.

[11] A. H. Saleh, A. E. Farag, and E. A. Eysa, "Reservoir quality of Abu Roash (G) member in Karama oil field, East Bahariya Concession, North Western Desert, Egypt," *Arabian Journal of Geosciences*, vol. 14, no. 3, pp. 1–18, 2021.

[12] R. H. Worden, P. J. Armitage, A. R. Butcher et al., "Petroleum reservoir quality prediction: overview and contrasting approaches from sandstone and carbonate communities," *Geological Society, London, Special Publications*, vol. 435, no. 1, pp. 1–31, 2018.

[13] M. K. Barakat and A. Z. Nooh, "Reservoir quality using the routine core analysis data of Abu Roash "C" in Badr El Din-15 oil field, Abu Gharadig basin, North Western Desert, Egypt," *Journal of African Earth Science*, vol. 129, pp. 683–691, 2017.

[14] E. A. Gawad, M. Fathy, M. Reda, and H. Ewida, "Source rock evaluation of the Central Gulf of Suez, Egypt: a 1D basin modelling and petroleum system analysis," *Geological Journal*, vol. 56, no. 7, pp. 3850–3867, 2021.

[15] E. A. Gawad, M. Fathy, M. Reda, and H. Ewida, "3D static reservoir modeling, using well logs and seismic data, to re-evaluate the oil potentiality of the Upper Rudeis Formation (Asl member) in October oil field, Gulf of Suez, Egypt," *Annals of the Geological Survey of Egypt, The Egyptian Mineral Resources Authority*, vol. XXXIIV, pp. 216–237, 2020.

[16] J. M. Hunt, *Petroleum Geochemistry and Geology*, Freeman and company, New York, 2nd edition, 1996.

[17] E. A. Gawad, M. Fathy, M. Reda, and H. Ewida, "Re-evaluation of the oil potentiality of Matulla Formation in October oil field, Gulf of Suez, Egypt, using the 3D static reservoir modeling of well logs and seismic data," *Egyptian Journal of Applied Geophysics, Egypt, Egyptian Society of Applied Petrophysics*, vol. 18, no. 2, pp. 21–34, 2019.

[18] M. I. Abdel-Fattah, S. Sen, S. M. Abuzied, M. Abioui, A. E. Radwan, and M. Benssaou, "Facies analysis and petrophysical investigation of the Late Miocene Abu Madi sandstones gas reservoirs from offshore Baltim east field (Nile Delta, Egypt)," *Marine and Petroleum Geology*, vol. 137, p. 105501, 2022.

[19] C. R. Selley, *Applied Sedimentology*, Academic Press, San Diego, 2nd edition, 2000.

[20] A. A. Shehata, M. A. Sarhan, M. I. Abdel-Fattah, and S. Mansour, "Geophysical assessment for the oil potentiality of the Abu Roash "G" reservoir in West Beni Suef Basin, Western Desert, Egypt," *Journal of African Earth Sciences*, vol. 199, p. 104845, 2023.

[21] Z. M. Abd-Allah, W. H. Abdullah, and M. I. Abdel-Fattah, "Assessment of Eocene, Paleocene and Cretaceous source rocks in the West Feiran area, offshore Gulf of Suez, Egypt," *Journal of Petroleum Science and Engineering*, vol. 180, pp. 756–772, 2019.

[22] J. Espitalie, G. Deroo, and F. Marquis, "La pyrolyse Rock-Eval et ses applications. Première partie," *Revue De L Institut Francais Du Petrole*, vol. 40, no. 5, pp. 563–579, 1985.

[23] A. F. Makky, M. I. El Sayed, A. S. A. El-Ata, I. M. Abd El-Gaied, M. I. Abdel-Fattah, and Z. M. Abd-Allah, "Source rock evaluation of some upper and lower cretaceous sequences, West Beni Suef concession, Western Desert, Egypt," *Egyptian Journal of Petroleum*, vol. 23, no. 1, pp. 135–149, 2014.

[24] A. Q. Mahdi, M. I. Abdel-Fattah, and H. A. Hamdan, "An integrated geochemical analysis, basin modeling, and palynofacies analysis for characterizing mixed organic-rich carbonate and shale rocks in Mesopotamian Basin, Iraq: insights for multi-source rocks evaluation," *Journal of Petroleum Science and Engineering*, vol. 216, article 110832, 2022.

[25] K. E. Peters, C. C. Walters, and J. M. Moldowan, *The Biomarker Guide, Biomarkers and Isotopes in Petroleum Exploration and Earth History*, vol. 2, Cambridge University Press, New York, 2005.

[26] G. M. Awad, "Habitat of oil in Abu Gharadig and Faiyum basins, Western Desert, Egypt," *AAPG Bulletin*, vol. 68, no. 5, pp. 564–573, 1984.

[27] N. H. Elgendy, A. A. Badr, and M. K. Barakat, "Petrophysical studies on Upper Bahariya and Abu Roash "G" reservoirs using well logs in Karama field, North Western Desert, Egypt," *Bulletin of Faculty of Science, Zagazig University*, vol. 2022, no. 2, pp. 57–70, 2022.

[28] M. Mahsoub, R. Abulnasr, M. Boukhary, M. Faris, and M. A. El Aal, "Bio- and sequence stratigraphy of Upper Cretaceous–Palaeogene rocks, East Bahariya Concession, Western Desert, Egypt," *Geologia Croatica*, vol. 65, no. 2, pp. 109–138, 2012.

[29] M. Abu El Naga, "Paleozoic and mesozoic depocenters and hydrocarbon generating areas, northern western desert: 7th egyptian general petroleum corporation exploration seminar," in *Exploration Seminar*, pp. 1–8, Cairo, 1984.

[30] M. A. Abdel Aal, "Tectonic evolution and hydrocarbon prospectivity of Abu Gharadig Basin, North Western Desert, Egypt," *Journal of Earth Sciences and Geotechnical Engineering*, vol. 8, no. 2, pp. 195–213, 2018.

[31] A. Badawy, I. El-Kassas, M. Sultan, and M. Salah, "Hydrocarbon prospectivity and exploration challenges of the Abu Gharadig Basin, North Western Desert, Egypt: a review," *Geosciences*, vol. 10, no. 1, p. 12, 2020.

[32] A. R. Moustafa, A. Saoudi, A. Moubasher, I. M. Ibrahim, H. Molokhia, and B. Schwartz, "Structural setting and tectonic evolution of the Bahariya depression, Western Desert, Egypt," *GeoArabia*, vol. 8, no. 1, pp. 91–124, 2003.

[33] A. M. El Gazzar, A. R. Moustafa, and P. Bentham, "Structural evolution of the Abu Gharadig field area, northern Western Desert, Egypt," *Journal of African Earth Sciences*, vol. 124, pp. 340–354, 2016.

[34] Q. R. Passey, K. M. Bohacs, W. L. Esch, R. Klimentidis, and S. Sinha, "A practical model for organic richness from porosity and resistivity logs," *AAPG Bulletin*, vol. 74, pp. 1777–1794, 1990.

[35] K. E. Peters, "Guidelines for evaluation petroleum source rock using programmed pyrolysis," *AAPG Bulletin*, vol. 70, pp. 318–329, 1986.

[36] G. Asquith and D. Krygowski, "*Basic well log analysis for geologists*," *AAPG Methods in Exploration Series*, vol. 16, 2004.

[37] M. Rider, *The Geological Interpretation of Well Logs*, Whittles Publishing, 1996.

[38] R. C. Selley, *Elements of Petroleum Geology*, Gulf Professional Publishing, 1998.

[39] D. Tiab and E. Donaldson, *Petrophysics: Theory and Practice of Measuring Reservoir Rock and Fluid Transport Properties*, Gulf Professional Publishing, 3rd edition, 2015.

[40] J. H. Doveton, *Principles of Mathematical Petrophysics*, Oxford University Press, 2014.

[41] S. B. A. Kelishami and R. Mohebian, "Petrophysical rock typing (PRT) and evaluation of Cenomanian–Santonian lithostratigraphic units in southwest of Iran," *Carbonates and Evaporites*, vol. 36, no. 1, p. 13, 2021.

[42] M. S. El Sharawy and B. S. Nabawy, "The role of gamma-ray logs in deciphering geochemical and geological aspects of the Rudeis Formation, Gulf of Suez, Egypt," *Arabian Journal of Geosciences*, vol. 11, no. 10, pp. 1–16, 2018.

[43] S. Lüning and S. Kolonic, "Uranium spectral gamma-ray response as a proxy for organic richness in black shales: applicability and limitations," *Journal of Petroleum Geology*, vol. 26, no. 2, pp. 153–174, 2003.

[44] B. P. Tissot and D. H. Welte, *Petroleum Formation and Occurrence*, Springer, Verlag, New York, 2nd edition, 1984.

[45] T. M. Smagala, A. C. Brown, and L. G. Nydedgger, "Log-derived indicator of thermal maturity, Niobrara Formation, Denver Basin, Colorada, Nebraska, Wyoming," in *Hydrocarbon Source Rocks of the Greater Rocky Mountain Region*, J. Woodward, F. F. Meissner, and J. S. Clayton, Eds., pp. 355–364, Association of Geologists, Rocky Mountain, 1984.

[46] H. Carvajal-Ortiz and T. Gentzis, "Critical considerations when assessing hydrocarbon plays using Rock-Eval pyrolysis and organic petrology data: data quality revisited," *International Journal of Coal Geology*, vol. 152, pp. 113–122, 2015.

[47] I. M. El-Mansey, M. G. Shehata, M. A. Massoud, and S. A. Awad, "Geochemical studies on subsurface Paleozoic sediments from some wells in Siwa-Faghur Basin, Western Desert, Egypt," *Egyptian Journal of Petroleum*, vol. 13, 2004.

[48] M. Gad, K. Dahab, and H. Ibrahim, "Applying of a geochemical model on the Nubian sandstone aquifer in Siwa Oasis, Western Desert, Egypt," *Environmental Earth Sciences*, vol. 77, no. 11, pp. 1–14, 2018.

[49] J. H. Hunt, *Petroleum Geochemistry and Geology*, W.H, Freeman, San Francisco, 1979.

[50] K. E. Peters and M. R. Cassa, "Applied source rock geochemistry," in *The Petroleum System-from Source to Trap*, L. B. Magoon and W. G. Dows, Eds., pp. 93–117, AAPG, Tulsa, OK, 1994.

[51] D. W. Waples, *Geochemistry in Petroleum Exploration*, International Human Resources Development Corporation, Boston, 1985.

[52] D. K. Baskin, "Atomic H/C ratio of kerogen as an estimate of thermal maturity and organic matter conversion," *AAPG Bulletin*, vol. 81, no. 9, pp. 1437–1450, 1997.

[53] J. Espitalie, L. Laporte, M. Madec et al., "Méthode rapide de caractérisation des roches mètres, de leur potentiel pétrolier et de leur degré d'évolution," *Revue de l'Institut Francais du Petrole*, vol. 32, no. 1, pp. 23–42, 1977.

[54] A. M. Burgan and C. A. Ali, "Characterization of the black shales of the Temburong Formation in West Sabah, East Malaysia," *European Journal of Scientific Research*, vol. 30, pp. 79–98, 2009.

[55] K. E. Peters, J. W. Snedden, A. Sulaeman, J. F. Sarg, and R. J. Enrica, "A new geochemical-sequence stratigraphic model for the Mahakam delta and Makassar slope, Kalimantan, Indonesia," *AAPG Bulletin*, vol. 84, pp. 12–44, 2000.

[56] G. Shanmugam, "Significance of coniferous rain forests and related organic matter in generating commercial quantities of oil, Gippsland basin, Australia," *AAPG Bulletin*, vol. 69, no. 8, p. 1241, 1985.

[57] T. G. Bevan and A. R. Moustafa, "Inverted rift-basins of northern Egypt," *Regional Geology and Tectonics*, vol. 2, pp. 483–506, 2012.

[58] J. C. Dolson, M. V. Shann, S. I. Matbouly, H. Hammouda, and R. M. Rashed, "Egypt in the twenty-first century: petroleum potential in offshore trends," *GeoArabia*, vol. 6, no. 2, pp. 211–230, 2001.

[59] A. R. Moustafa, "Mesozoic-Cenozoic basin evolution in the northern Western Desert of Egypt," *Geology of East Libya*, vol. 3, pp. 29–46, 2008.

[60] W. Bosworth, A. S. El-Hawat, D. E. Helgeson, and K. Burke, "Cyrenaican "shock absorber" and associated inversion strain shadow in the collision zone of Northeast Africa," *Geology*, vol. 36, no. 9, pp. 695–698, 2008.

[61] EGPC, "Western desert, oil and gas fields, a comprehensive overview, 11th EGPC Conf," in *A Comprehensive Overview, 11th EGPC Conf.*, p. 4310, Cairo, 1992.

[62] J. H. Hunt, *Petroleum Geochemistry and Geology*, W. H. Freeman, New York, 1995.

[63] H. Dembicki, "Three common source rock evaluation errors made by geologists during prospect or play appraisals," *AAPG Bulletin*, vol. 93, no. 3, pp. 341–356, 2009.

[64] K. S. Jackson, P. J. Hawkins, and A. J. R. Bennett, "Regional facies and geochemical evaluation of southern Denison Trough," *APEA Journal*, vol. 20, no. 1, pp. 143–158, 1985.

[65] K. E. Peters, T. H. Fraser, W. Amris, B. Rustanto, and E. Hermanto, "Geochemistry of crude oils from eastern Indonesia," *AAPG Bulletin*, vol. 83, pp. 1927–1942, 1999.

[66] M. Obermajer, M. G. Fowler, and L. R. Snowdon, "Depositional environment and oil generation in Ordovician source rocks from southwestern Ontario, Canada: organic geochemical and petrological approach," *AAPG Bulletin*, vol. 83, no. 9, pp. 1426–1453, 1999.